Circulation Research
JOURNAL OF THE AMERICAN HEART ASSOCIATION

Local Control of Nuclear Calcium Signaling in Cardiac Myocytes by Perinuclear Microdomains of Sarcolemmal Insulin-Like Growth Factor 1 Receptors

Cristian Ibarra, Jose M. Vicencio, Manuel Estrada, Yingbo Lin, Paola Rocco, Paola Rebellato, Juan P. Munoz, Jaime Garcia-Prieto, Andrew F.G. Quest, Mario Chiong, Sean M. Davidson, Ivana Bulatovic, Karl-Henrik Grinnemo, Olle Larsson, Gyorgy Szabadkai, Per Uhlén, Enrique Jaimovich and Sergio Lavandero

Circ Res. 2013;112:236-245; originally published online November 1, 2012;
doi: 10.1161/CIRCRESAHA.112.273839
Circulation Research is published by the American Heart Association, 7272 Greenville Avenue, Dallas, TX 75231

Print ISSN: 0009-7330. Online ISSN: 1524-4571

Local Control of Nuclear Calcium Signaling in Cardiac Myocytes by Perinuclear Microdomains of Sarcolemmal Insulin-Like Growth Factor 1 Receptors

Cristian Ibarra,* Jose M. Vicencio,* Manuel Estrada, Yingbo Lin, Paola Rocco, Paola Rebellato, Juan P. Munoz, Jaime Garcia-Prieto, Andrew F.G. Quest, Mario Chiong, Sean M. Davidson, Ivana Bulatovic, Karl-Henrik Grinnemo, Olle Larsson, Gyorgy Szabadkai, Per Uhlén,* Enrique Jaimovich,* Sergio Lavandero*

***Rationale*: The ability of a cell to independently regulate nuclear and cytosolic Ca^{2+} signaling is currently attributed to the differential distribution of inositol 1,4,5-trisphosphate receptor channel isoforms in the nucleoplasmic versus the endoplasmic reticulum. In cardiac myocytes, T-tubules confer the necessary compartmentation of Ca^{2+} signals, which allows sarcomere contraction in response to plasma membrane depolarization, but whether there is a similar structure tunneling extracellular stimulation to control nuclear Ca^{2+} signals locally has not been explored.**

***Objective*: To study the role of perinuclear sarcolemma in selective nuclear Ca^{2+} signaling.**

***Methods and Results*: We report here that insulin-like growth factor 1 triggers a fast and independent nuclear Ca^{2+} signal in neonatal rat cardiac myocytes, human embryonic cardiac myocytes, and adult rat cardiac myocytes. This fast and localized response is achieved by activation of insulin-like growth factor 1 receptor signaling complexes present in perinuclear invaginations of the plasma membrane. The perinuclear insulin-like growth factor 1 receptor pool connects extracellular stimulation to local activation of nuclear Ca^{2+} signaling and transcriptional upregulation through the perinuclear hydrolysis of phosphatidylinositol 4,5-biphosphate inositol 1,4,5-trisphosphate production, nuclear Ca^{2+} release, and activation of the transcription factor myocyte-enhancing factor 2C. Genetically engineered Ca^{2+} buffers—parvalbumin—with cytosolic or nuclear localization demonstrated that the nuclear Ca^{2+} handling system is physically and functionally segregated from the cytosolic Ca^{2+} signaling machinery.**

***Conclusions*: These data reveal the existence of an inositol 1,4,5-trisphosphate–dependent nuclear Ca^{2+} toolkit located in direct apposition to the cell surface, which allows the local control of rapid and independent activation of nuclear Ca^{2+} signaling in response to an extracellular ligand. (*Circ Res.* 2013;112:236-245.)**

Key Words: cardiomyocytes ■ excitation–contraction coupling ■ formamide ■ interorganelle communication ■ methyl-β-cyclodextrin ■ parvalbumin ■ pre–T-tubules

Throughout the past 2 decades, intense research has linked nuclear Ca^{2+} signals to a wide range of physiological and pathological cellular responses.[1,2] Although nuclear Ca^{2+} is essential for processes such as nuclear transport, chromatin condensation, and the activation of several transcription factors,[3–6] the origin of the nuclear Ca^{2+} signal is still controversial. Some authors suggest that nuclear Ca^{2+} signals can result from Ca^{2+} release that initiates in the cytosol and then propagates to the nucleus,[7,8] whereas others suggest that it occurs independently of cytosolic Ca^{2+} release.[9,10] Consistent with the latter notion, we have previously reported that stimulation of the insulin-like growth factor 1 receptor (IGF-1R) triggers a rapid inositol 1,4,5-trisphosphate (IP_3)–dependent

Original received May 22, 2012; revision received October 26, 2012; accepted October 31, 2012. In September 2012, the average time from submission to first decision for all original research papers submitted to *Circulation Research* was 11.5 days.

From the Centro de Estudios Moleculares de la Célula, Facultad de Ciencias Quimicas y Farmaceuticas and Facultad de Medicina (C.I., J.M.V., M.E., P.R., J.P.M., A.F.G.Q., M.C., E.J., S.L.) and Instituto de Ciencias Biomédicas, Facultad de Medicina (M.E., A.F.G.Q., E.J., S.L.), Universidad de Chile, Santiago, Chile; Department of Medical Biochemistry and Biophysics, Karolinska Institutet, Stockholm, Sweden (C.I., P.R., P.U.); Department of Cell and Developmental Biology (J.M.V., G.S.) and Hatter Cardiovascular Institute (J.M.V., J.G-P., S.M.D.), University College London, London, United Kingdom; Department of Biomedical Sciences (G.S.), University of Padua, Padua, Italy; Department of Oncology and Pathology, Karolinska Institutet, Cancer Center Karolinska (Y.L., O.L.) and Department of Molecular Medicine and Surgery, Division of Cardiothoracic Surgery and Anesthesiology, Karolinska Institutet (I.B., K-H.G.), Karolinska University Hospital, Stockholm, Sweden; and Department of Internal Medicine (Cardiology Division), University of Texas Southwestern Medical Center, Dallas, TX (S.L.).

*These authors equally contributed to this work.

The online-only Data Supplement is available with this article at http://circres.ahajournals.org/lookup/suppl/doi:10.1161/CIRCRESAHA.112.273839/-/DC1.

Correspondence to Sergio Lavandero, Centro de Estudios Moleculares de la Celula, Facultad de Ciencias Quimicas y Farmaceuticas/Facultad de Medicina, Universidad de Chile, Sergio Livingstone 1007, CL-838049, Santiago, Chile (e-mail slavander@uchile.cl); Enrique Jaimovich, Centro de Estudios Moleculares de la Celula, Facultad de Medicina, Universidad de Chile, Independencia 1027, CL-88389100 Santiago, Chile (e-mail ejaimovi@med.uchile.cl); or Per Uhlén, Department of Medical Biochemistry, Karolinska Institutet, SE-17177 Stockholm, Sweden (e-mail per.uhlen@ki.se).

Non-standard Abbreviations and Acronyms	
IGF-1	insulin-like growth factor 1
IGF-1R	IGF-1 receptor
IP_3	inositol 1,4,5-trisphosphate
IP_3R	IP_3 receptor
MEF2C	myocyte enhancing factor 2C
PLC	phospholipase C

Ca^{2+} signal that originates in the nucleus and then propagates to the cytosol of cultured cardiac myocytes.[11] These results raised the question of how the activation of a plasma membrane receptor is able to elicit an IP_3-dependent response in the nucleus, bypassing IP_3 receptors (IP_3R) present in the peripheral sarcoplasmic reticulum. The generally accepted explanation is that IP_3 diffuses rapidly and that a higher abundance in the nucleoplasmic reticulum of specific IP_3R isoforms with increased sensitivity to IP_3 accounts for the speed and independence of the nuclear Ca^{2+} signals.[12] The cellular architecture of cardiac myocytes, however, suggests an alternative scenario. In these cells, T-tubules consist of plasma membrane invaginations toward internal sarcoplasmic reticulum, forming the well-known microdomains for excitation–contraction coupling.[13] Is it possible that these structures could also contribute to spatially restrict the generation of nuclear Ca^{2+} signals in response to extracellular stimulation? We addressed this question by studying perinuclear sarcolemmal invaginations that contain the IGF-1R signaling complex, leading to a nuclear Ca^{2+} increase that is fully independent of cytosolic Ca^{2+} and regulates transcription by physically bringing a plasma membrane receptor in close proximity to the nucleus.

In This Issue, see p 223
Editorial, see p 224

Methods

Primary cardiac myocytes were purified, as previously described, from neonatal rats,[14] adult rats,[15,16] adult mice,[16–18] or human embryos.[19] The

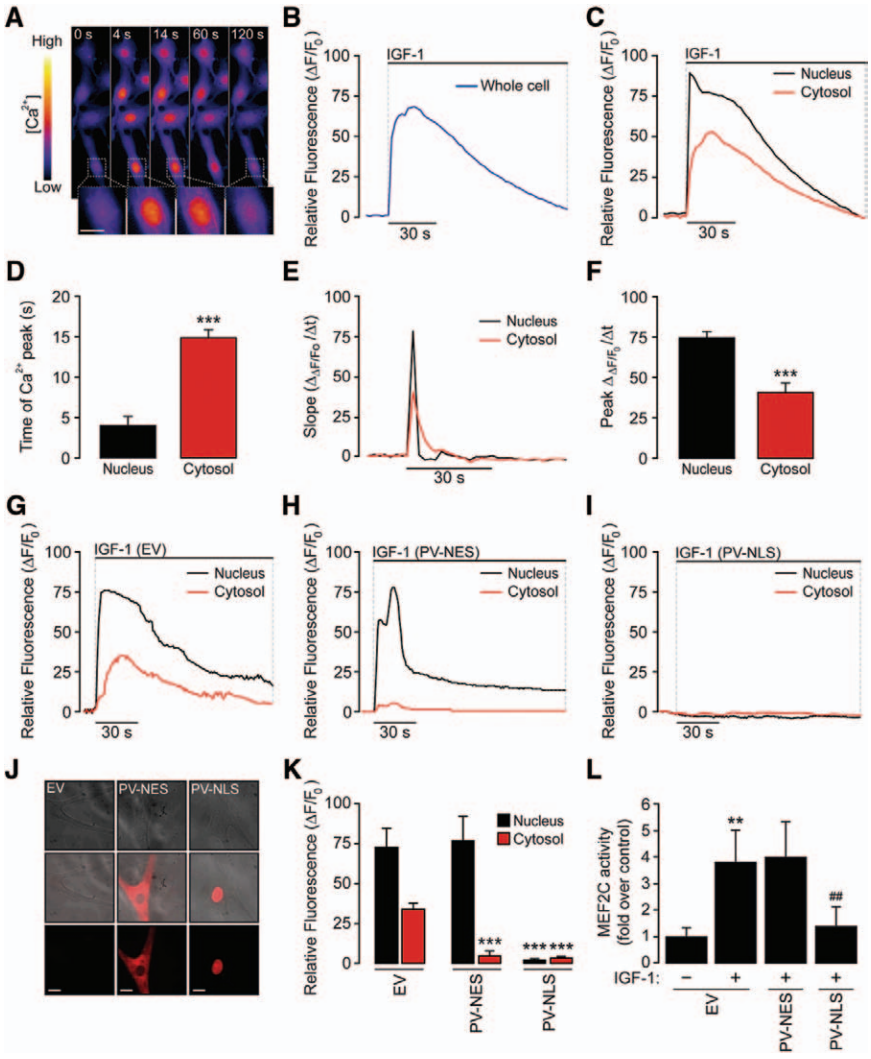

Figure 1. Nuclear compartmentation of Ca^{2+} signaling triggered by extracellular insulin-like growth factor 1 (IGF-1) in neonatal rat cardiomyocytes. A, Dynamic Ca^{2+} imaging of primary neonatal rat cardiac myocytes (CM) loaded with fluo-3AM and stimulated with 10 nmol/L IGF-1 in Ca^{2+}-free recording medium. **B**, The whole-cell Ca^{2+} signal triggered by IGF-1 stimulation of CM loaded with fluo-3AM (n=12). **C**, Analysis of relative fluorescence intensity in nuclear and cytosolic regions. **D**, Quantification of time to peak [Ca^{2+}] in the nucleus vs the cytosol (n=12, statistical significance was calculated by *t* test, ***P<0.001, values are expressed as mean±SEM). **E**, The rate of Ca^{2+} increase in nuclear and cytosolic compartments was obtained by calculating the derivative of the Ca^{2+} signal over time. **F**, Quantification of the peak rate of Ca^{2+} increase in nuclear and cytosolic compartments (n=12, statistical significance was evaluated by *t* test, ***P<0.001 between compartments, values are expressed as mean±SEM). **G** to **I**, Relative fluorescence intensity of CM transfected with empty vector (EV), cytosolic parvalbumin-nuclear exclusion signal (PV-NES), or nuclear parvalbumin-nuclear localizing signal (PV-NLS) as indicated and stimulated with IGF-1 in Ca^{2+}-free recording medium. **J**, DsRed/bright field images of CM transfected with EV, PV-NES, or PV-NLS as indicated. **K**, Summary of peak fluorescence values after IGF-1 stimulation of CM expressing EV, PV-NES, or PV-NLS as indicated (n=12, 1-way ANOVA, ***P<0.001 vs EV-transfected cells, values are expressed as mean±SEM). **L**, Myocyte-enhancing factor 2C reporter activity of cells expressing EV, PV-NES, or PV-NLS as indicated and stimulated with IGF-1 for 24 hours (n=6, 2-way ANOVA, **P<0.01 vs untreated cells and ##P<0.01 vs EV-treated cells, values are expressed as mean±SEM). White bar, 10 μm.

Ethical Committee of the Karolinska University Hospital approved the use of cells from surgically aborted human tissue. This investigation conforms to the principles outlined in the Declaration of Helsinki. Dynamic Ca^{2+} imaging was performed on fluo-3AM–loaded cardiac myocytes, using an inverted fluorescence microscope for whole-cell images or a confocal inverted microscope for line scan analysis. Ca^{2+} and IP_3 measurements were conducted in HEPES-buffered recording saline, either with or without Ca^{2+} as indicated. Overexpression was carried out using standard lipofectamine transfection and adenoviral transduction protocols. All colocalization analyses were performed on deconvolved confocal images using the software ImageJ or Imaris. Subcellular fractionation was performed by differential centrifugation. Immunoprecipitation was performed using protein G sepharose beads. Intracellular IP_3 mass measurements were performed by radioligand binding assays. Sucrose gradient fractioning was performed on cardiac myocytes maintained for 24 hours in ^{14}C-cholesterol. Lipid raft disruption was performed by acute treatment with the cholesterol-binding reagent methyl-β-cyclodextrin (MβCD). T-tubule disruption was induced by osmotic shock with formamide. Three-dimensional rendering of images was performed on Z-stacks of 0.1-μm thick confocal images using Imaris software. Statistical significance was evaluated by 1- or 2-way ANOVA, according to experimental conditions. Fully detailed methods are available in the Online Data Supplement.

Results

IGF-1 Triggers a Fast and Cytosol-Independent Nuclear Ca^{2+} Signal

Primary neonatal rat cardiac myocytes were stimulated with IGF-1, and a rapid Ca^{2+} signal was observed (Figure 1A and 1B and Online Movie I). The kinetics of the Ca^{2+} signal were faster in the nucleus than in the cytosol, increasing to a maximum within 4 seconds in the nucleus, whereas cytosolic Ca^{2+} reached a maximum at 14 seconds (Figure 1C and 1D). The initial rate of Ca^{2+} increase, corresponding to the derivative of the Ca^{2+} signal over time, was double in the nucleus compared with the cytosol (Figure 1E and 1F). To evaluate the contribution of nuclear Ca^{2+} to the whole signal, we studied the effects of IGF-1 in cells expressing the Ca^{2+}-buffering protein parvalbumin localized to either the cytosol by means of a parvalbumin-nuclear exclusion signal or to the nucleus by a parvalbumin-nuclear localizing signal (Figure 1J).[20] When cytosolic Ca^{2+} was buffered, IGF-1 treatment led to an increase in nuclear Ca^{2+} exclusively (Figure 1H and 1K), whereas in cardiac myocytes with nuclear Ca^{2+} buffering, no response in intracellular Ca^{2+} was observed, either in the nucleus or in the cytosol (Figure 1I and 1K). These results excluded the possibility of dye-localization artifacts and revealed that the nuclear component of the Ca^{2+} signal occurs not only more rapidly but also independently of the cytosolic signal. To determine the functional relevance of such Ca^{2+} compartmentation, we selectively buffered nuclear Ca^{2+} and monitored the activation of the Ca^{2+}-dependent transcription factor myocyte-enhancing factor 2C (MEF2C).[3] Treatment for 24 hours with IGF-1 significantly increased the MEF2C reporter activity in control cells (empty vector, EV) and in cells expressing parvalbumin-nuclear exclusion signal, whereas in cells expressing parvalbumin-nuclear localizing signal the reporter activity was abolished (Figure 1L). Thus, the IGF-1–induced Ca^{2+} response in the nucleus, not the cytosol, is critical for the activity of the target transcription factor MEF2C, which is consistent with the primarily nuclear effects of IGF-1 that we observed on cellular Ca^{2+}. Remarkably, using human embryonic cardiac myocytes, we also observed that the Ca^{2+} signal triggered by IGF-1 was faster in the nucleus, followed by the cytosolic component (Figure 2A and 2B), whereas the basal oscillations of Ca^{2+} in these cells were mainly initiated in the cytosol and then followed by the nuclear Ca^{2+} increase (Figure 2C and 2D). We additionally used adult rat cardiac myocytes to study whether this signal was present after cardiac development and differentiation. In these cells, there was also a strong and fast Ca^{2+} signal after IGF-1 addition (Figure 2E), with higher amplitude (and shorter time to peak) in the nucleus than the cytosol (Figure 2F). The persistence of this signal in medium without Ca^{2+} indicates its release from intracellular stores

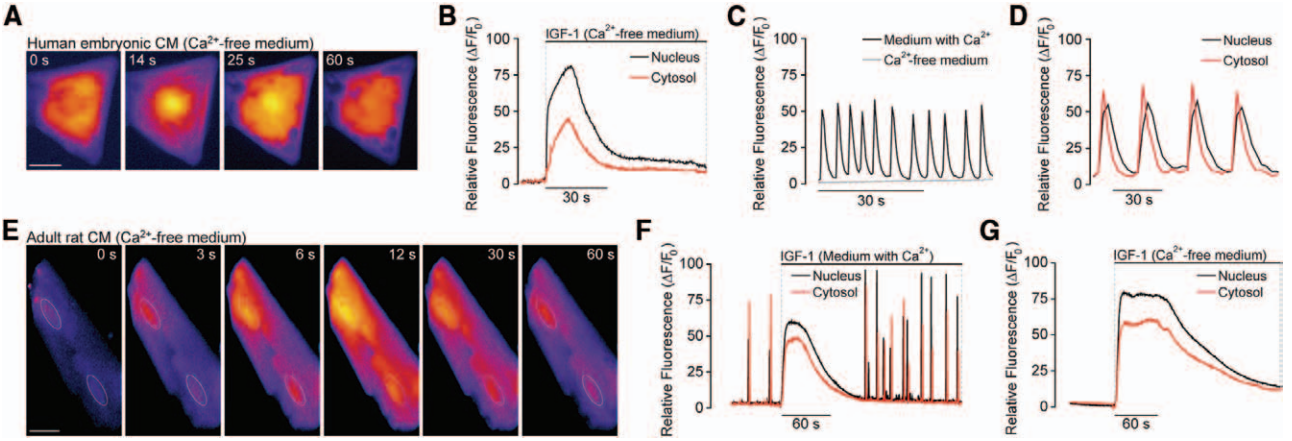

Figure 2. Nuclear Ca^{2+} signaling triggered by insulin-like growth factor 1 (IGF-1) in human embryonic cardiac myocytes and adult rat cardiac myocytes. A, Dynamic Ca^{2+} imaging of human embryonic cardiac myocytes (heCM) loaded with fluo-4AM and stimulated with 10 nmol/L IGF-1 in Ca^{2+}-free recording medium. **B**, Analysis of the relative fluorescence intensity in nuclear and cytosolic regions of interest (ROIs) from the images in **A**. **C**, The whole-cell basal Ca^{2+} oscillations of heCM maintained in Ca^{2+}-containting recording medium (black line) or in Ca^{2+}-free recording medium (gray line). **D**, Analysis of the relative fluorescence intensity in nuclear and cytosolic ROIs from the signals in **C** (n=2). **E**, Dynamic Ca^{2+} imaging of adult rat cardiac myocytes (arCM) loaded with fluo-3AM and stimulated with 50 nmol/L IGF-1 in Ca^{2+}-free recording medium. **F**, Analysis of the relative fluorescence intensity in nuclear and cytosolic ROIs of arCM stimulated with 50 nmol/L IGF-1 in recording medium with Ca^{2+}. **G**, Analysis of the relative fluorescence intensity in nuclear and cytosolic ROIs of arCM stimulated with 50 nmol/L IGF-1 in Ca^{2+}-free recording medium. Experiments with human embryonic cardiac myocytes and adult rat cardiac myocytes are representative of 2 cultures and 4 independent cultures, respectively.

(Figure 2G), in agreement with our observations in neonatal rat cardiac myocytes and human embryonic cardiac myocytes.

IGF-1R Is Distributed in the Perinuclear Zone of Cardiac Myocytes

Based on the above results, we investigated whether the nuclear Ca^{2+} response is triggered by an IGF-1R signaling complex present in close physical proximity to the nucleus. Confocal immunofluorescence studies in permeabilized neonatal cells revealed a high level of both α- and β-subunits of the IGF-1R in the perinuclear area, as evidenced by counterstaining with the nuclear lamina protein lamina-associated protein 2 (Figure 3A and 3B). To eliminate the possibility that perinuclear staining was a result of IGF-1R internalization, we performed studies on nonpermeabilized cells using an antibody that recognizes an extracellular epitope of the IGF-1R α-subunit. Lamina-associated protein 2 antibodies did not stain the nuclear envelope in these nonpermeabilized cells (Online Figure IA), and the intactness of the plasma membrane was verified further by the absence of nuclear staining with the vital dye, propidium iodide (Online Figure IB and IC). Three-dimensional rendering of images obtained from fixed nonpermeabilized cardiac myocytes revealed details of the IGF-1Rα distribution surrounding the nucleus (Figure 3C and Online Movie II). To exclude fixation or labeling artifacts, we transfected cells with IGF-1R–green fluorescent protein and studied living cardiac myocytes. We observed a corresponding perinuclear distribution of the IGF-1R, which additionally projected through the nucleus (Figure 3D and Online Movie III). We performed similar studies in adult rat cardiac myocytes. Using fixed permeabilized cells, we observed a clear perinuclear staining of the IGF-1Rα, in addition to a sarcolemmal striated pattern (Online Figure IIA–IIC). Importantly, when studying fixed, nonpermeabilized cells, we also observed a sarcolemmal distribution of the IGF-1Rα in the perinuclear zone (Figure 3E). We controlled our permeabilization protocols by monitoring propidium iodide incorporation (Online Figure IID). Biochemical fractionations confirmed these results in neonatal and adult cells, in which both α- and β-subunits of endogenous IGF-1R were detected in the membrane fractions as expected, but most interestingly, the nuclear fraction also revealed the presence of mature IGF-1R α- and β-subunits (Figure 3F and 3G). Of note, the immature pre–IGF-1R peptide, which is formed by both α- and β-subunits and transits through the biosynthetic pathway, was detected in the membrane fraction (microsomal) but not in the nuclear fraction. This additionally indicates that the

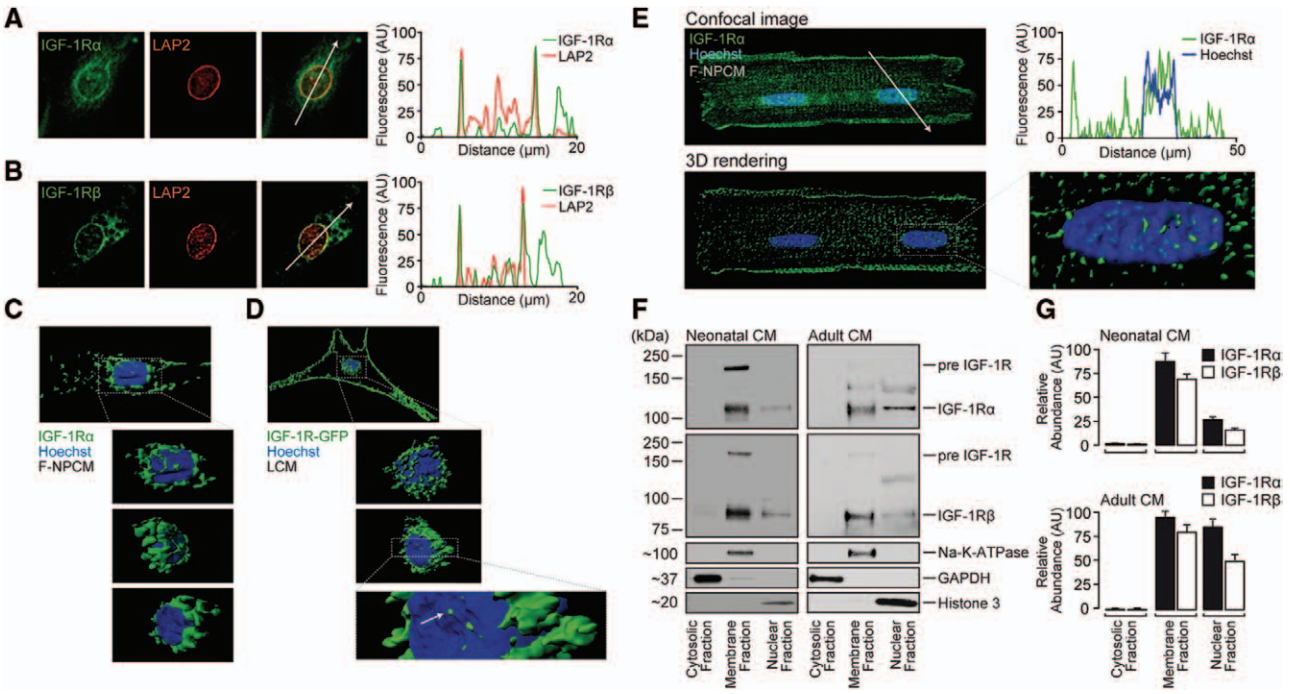

Figure 3. Perinuclear localization of the insulin-like growth factor 1 receptor (IGF-1R). A, Single-plane confocal images of immunostaining for IGF-1Rα/lamina-associated protein 2 (LAP2) on permeabilized cardiac myocytes (CM); a linear fluorescence profile is shown (n=3). **B**, Single-plane confocal immunostaining of IGF-1Rβ/LAP2 on permeabilized CM; a linear fluorescence profile analysis is shown. **C**, High-resolution 3-dimensional (3D) rendering from confocal images of immunofluorescence performed with antibodies against an extracellular epitope of the IGF-1Rα on fixed nonpermeabilized cardiac myocytes (fixed nonpermeabilized CM [F-NPCM]) counterstained with Hoechst 33342; a magnified rotation of perinuclear IGF-1Rα is shown at different angles of view. **D**, 3D image rendering from confocal stacks of living cardiac myocytes (LCM) expressing IGF-1R–green fluorescent protein (GFP) and stained with Hoechst 33342; a magnified rotation of perinuclear IGF-1R–GFP is shown at different angles of view; **white arrows** indicate IGF-1R–GFP structures that elongate across the nucleus. **E, Upper left**, Partial Z-stack confocal images of immunostaining for IGF-1Rα on fixed nonpermeabilized adult rat CM counterstained with Hoechst 33342. **Upper right**, A linear fluorescence profile is shown. **Lower left**, High-resolution 3D rendering from the cell shown above; a magnified perinuclear IGF-1Rα is shown. **F**, Western blot analysis of cytosolic membrane and nuclear subcellular fractions of primary neonatal or adult CM, as indicated. **G**, Quantification of IGF-1R α- and β-protein levels in the different subcellular fractions. Data are expressed as mean±SEM from 3 independent experiments.

mature plasma membrane forms (α: 125 kDa and β: 90 kDa) are the ones present in the nuclear fraction.

Perinuclear IGF-1R Is Part of Sarcolemmal Invaginations

Cardiac myocytes are composed of plasma membrane invaginations. To investigate whether sarcolemmal structures might provide a physical platform facilitating the fast nuclear events in response to extracellular IGF-1, we used a nonpermeable lipophilic plasma membrane labeling and observed a similar perinuclear staining to that observed for the IGF-1R in neonatal cells (Online Figure IIIA). Three-dimensional rendering obtained from high-resolution confocal stacks showed plasma membrane structures surrounding and projecting inside the nuclei of cultured cells (Online Figure IIIA, bottom). Remarkably, fluorescently labeled, cell-impermeable albumin (BSA-fluorescein isothiocyanate) was observed to diffuse quickly (2 minutes) into nuclear tunnels (Online Figure IV), indicating that extracellular medium is able to reach close nuclear proximity. To verify that the IGF-1R was present in these structures, we transfected IGF-1R–green fluorescent protein and labeled the plasma membrane in living cells. The IGF-1R and the plasma membrane showed consistent perinuclear colocalization (Figure 4A). Three-dimensional rendering analysis indicated that the IGF-1R was directly apposed to perinuclear sarcolemma (Figure 4A, bottom and Online Movie IV). In adult rat cardiac myocytes stained with cell mask, we also observed T-tubules extending from the cell surface to the nuclear envelope, where they established close contacts between the sarcolemma and the nucleus (Figure 4B). Equivalent results were obtained in adult mouse cardiac myocytes using the potentiometric dye Di-8-ANEPPS (Online Figure IIIB). Altogether, these results indicate that the IGF-1R is part of perinuclear sarcolemmal invaginations.

Pre–T-Tubules Contain the IGF-1R in Neonatal Cardiac Myocytes

In neonatal cardiac myocytes, the T-tubule system is not fully developed. To study the functional properties of the sarcolemmal invaginations that we observed in neonatal cells, we performed a protocol for the acute disruption of T-tubules by osmotic shock with formamide,[21] which does not disturb other cellular functions. In control cells, the T-tubule protein α1C subunit of L-type Ca^{2+} channels colocalized with the IGF-1R and lamina-associated protein 2 (Online Figure VA and VB), but in cells treated with formamide, the perinuclear distribution of α1C was disrupted (Figure 5A). Control cells displayed spontaneous, high-amplitude Ca^{2+} oscillations that were synchronized in the nuclear and cytosolic compartments, but in formamide-treated cells, both the amplitude and the synchronization of oscillations were lost (Figure 5B). Importantly, in these cells, the nuclear Ca^{2+} signal triggered by IGF-1 was abrogated (Figure 5C). Interestingly, these invaginations also exhibited characteristics of lipid rafts. The IGF-1R and caveolin 3 showed consistent perinuclear colocalization (Figure 5D), and sucrose gradient fractionations confirmed the abundance of both proteins in the same fractions (Figure 5E). These fractions also exhibited high levels of cholesterol (Figure 5F), which is an obligate component of lipid rafts and T-tubules.[22] Treatment of cardiac myocytes with the cholesterol-binding agent MβCD is known to abrogate the function and structure of lipid rafts.[23] Accordingly, MβCD decreased the levels of cholesterol in these fractions (Figure 5F) and, most importantly, abolished the nuclear Ca^{2+} response to IGF-1 (Figure

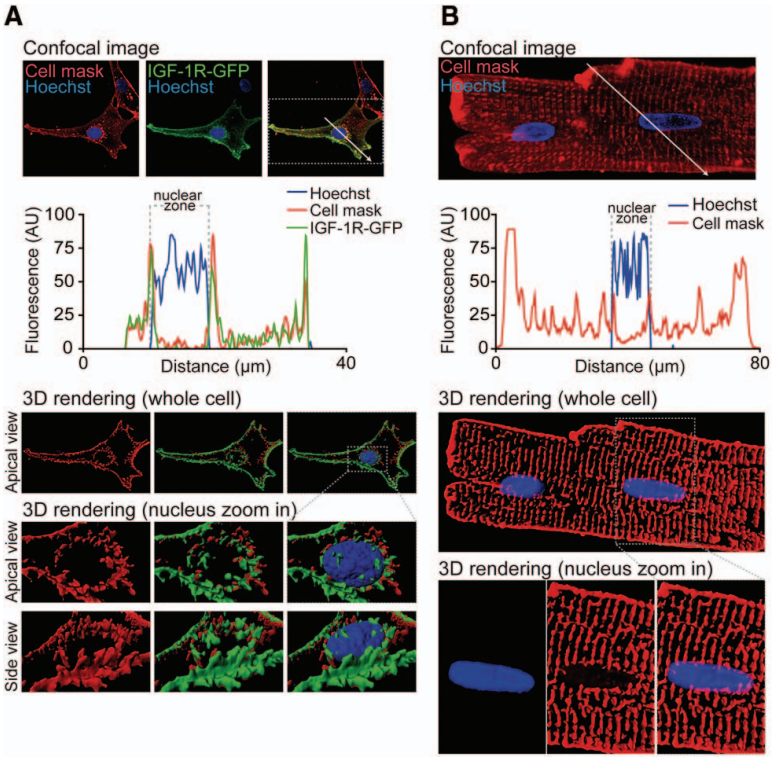

Figure 4. Perinuclear plasma membrane invaginations contain insulin-like growth factor 1 receptor (IGF-1R). A, Confocal stack images from living neonatal cardiac myocytes expressing IGF-1R–green fluorescent protein (GFP) and stained with Hoechst 33342 for 15 minutes and the plasma membrane stain Cell mask for 5 minutes before imaging; the **arrow** denotes a linear fluorescence profile analysis, shown in the **middle**; the dotted box denotes the zone used for a 3-dimensional (3D) rendering of 100 confocal planes, shown in the **bottom** (whole cell) with magnified views from different angles of the nucleus (**bottom**). **B,** Confocal Z-stack images of live adult rat cardiac myocytes stained with Hoechst 33342 for 15 minutes and the plasma membrane stain Cell mask for 5 minutes before imaging (**top**); the **arrow** denotes a linear fluorescence profile analysis, shown in the **middle**; a high-resolution 3D rendering of a partial Z-stack is shown for the whole cell, and the dotted box denotes the magnified views of the nucleus (**bottom**).

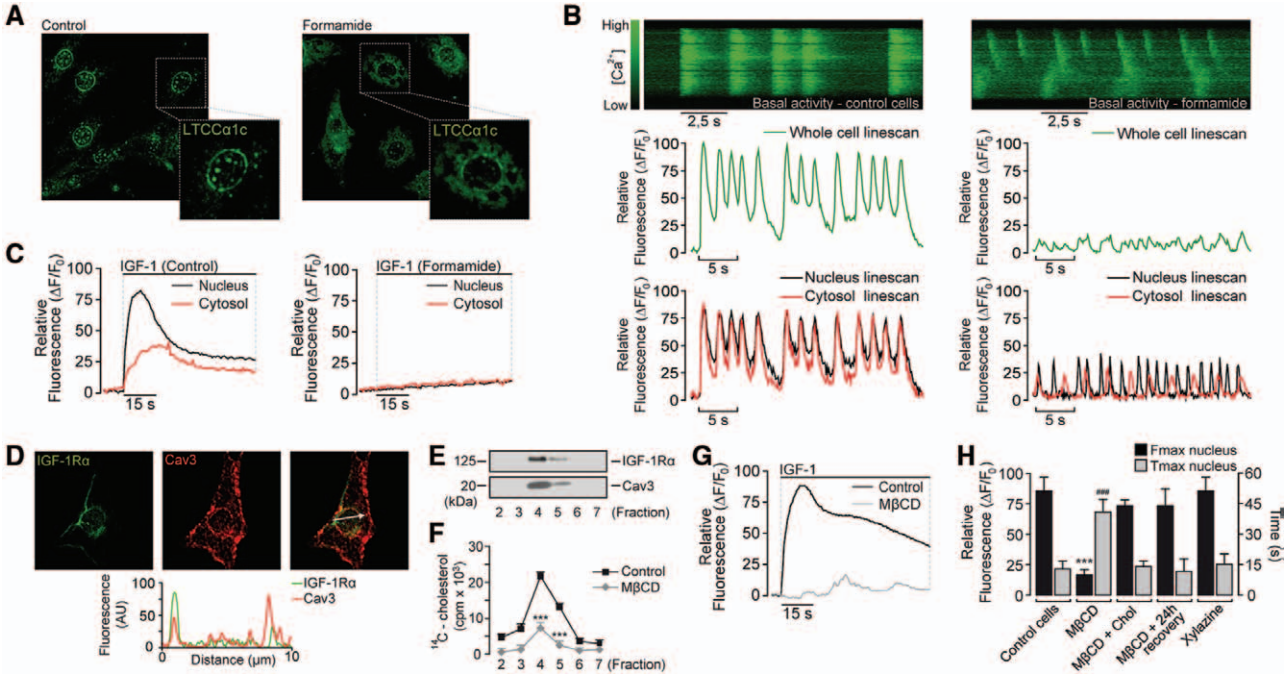

Figure 5. Disruption of perinuclear invaginations abrogates the effects of insulin-like growth factor 1 (IGF-1) on nuclear Ca^{2+}. A, Two-dimensional (2D) stack images from confocal immunofluorescence performed with antibodies against the α1c subunit of L-type Ca^{2+} channel (LTCCα1c) on fixed, nonpermeabilized cardiac myocytes previously subjected to acute T-tubule disruption by osmotic shock (formamide) or treated with vehicle (control). **B**, Neonatal rat cardiac myocytes were subjected to acute disruption of T-tubules by osmotic shock with formamide, followed by the recording of basal Ca^{2+} oscillations via confocal line scan analysis using fluo-3AM to monitor the functionality of T-tubules; relative fluorescence of whole-cell and nuclear vs cytosol regions is shown. Images are representative of independent triplicates. **C**, Ca^{2+} levels were registered in response to 10 nmol/L IGF-1, using cardiac myocytes treated with formamide or vehicle (control). **D**, Single-plane confocal images of immunofluorescence performed with antibodies against IGF-1Rα and caveolin-3 (Cav3) on permeabilized cardiac myocytes; the **arrow** denotes a linear fluorescence profile analysis of colocalization, shown in the **bottom**. **E**, Cardiac myocytes were subjected to sucrose gradient fractionation and analyzed by Western blot using antibodies against IGF-1Rα and Cav3. **F**, A 24-hour pulse of ^{14}C-cholesterol was applied to cardiac myocytes in culture, and acute disruption of lipid rafts was then performed by treatment with vehicle (control) or methyl-β-cyclodextrin (MβCD); cells were then subjected to sucrose fractionation, and the fractions were analyzed by liquid scintillation count to analyze cholesterol incorporation (values are expressed as mean±SEM of 3 independent experiments; statistical significance was evaluated by Student *t* test and expressed as $^{***}P<0.001$ vs control cells). **G**, Whole-cell Ca^{2+} measurements were performed on cardiac myocytes previously subjected to acute disruption of lipid rafts by treatment with the cholesterol-binding agent MβCD for 30 minutes, before imaging and stimulation with 10 nmol/L IGF-1 in Ca^{2+}-free medium. **H**, Summary of the peak fluorescence values (F_{max}, black bars) and the time elapsed to the $[Ca^{2+}]$ peak (T_{max}, gray bars) after IGF-1 stimulation of cardiac myocytes in Ca^{2+}-free medium that were pretreated as indicated (n=3, values are expressed as mean±SEM, the statistical significance was evaluated by 1-way ANOVA and expressed as $^{***}P<0.001$ vs F_{max} of control cells and $^{\#\#\#}P<0.001$ vs T_{max} of control cells).

5G and 5H and Online Figure VIA). We performed a series of controls to validate these results, in which we observed that cholesterol-inactivated MβCD did not affect the nuclear Ca^{2+} response (Figure 5H and Online Figure VIB), and the same was observed by giving the cells a 24-hour recovery period after the acute treatment with MβCD (Figure 5H and Online Figure VIC). Similarly, the Ca^{2+} signal was not affected by the nonspecific lipid-binding agent xylazine (Figure 5H and Online Figure VID). These results confirm that sarcolemmal invaginations with mixed characteristics of lipid rafts and T-tubules are present in neonatal cells and are necessary for excitation–contraction coupling and also for IGF-1R signaling to the nucleus. Although these pre–T-tubules do not form a continuous network, they serve as a functional perinuclear platform for the IGF-1R.

Signaling Pathway Downstream of the IGF-1R Is Compartmented in Perinuclear Microdomains

We addressed whether the perinuclear IGF-1R and the appropriate downstream Ca^{2+} signaling components share the same localization. The IGF-1R has dual properties, signaling through both its intrinsic tyrosine kinase activity and also through coupled heterotrimeric G-proteins, which activate phospholipase C (PLC) and catalyze cleavage of phosphatidylinositol 4,5-biphosphate (PIP_2) to produce IP_3, leading to Ca^{2+} signaling.[11,24] Accordingly, we observed that $G\alpha_i$ protein was highly colocalized with the IGF-1R in nuclear and perinuclear regions (Figure 6A). We performed immunoprecipitation experiments and detected both $G\alpha_i$ and Gβ subunits in IGF-1Rβ immunoprecipitates; this interaction was stronger in cells incubated with IGF-1 (Figure 6B). As expected, we observed a significant increase in intracellular IP_3 levels generated in response to IGF-1 in control cells, but not in cells expressing β-adrenergic receptor kinase carboxy terminal peptide (βARKct), which sequesters Gβγ dimmers (Figure 6C). To determine the subcellular localization of IP_3 production, we used cells expressing a plasma membrane–targeted yellow fluorescent protein-pleckstrin homology $domain_{PLC\delta}$ reporter, which binds to the IP_3 precursor PIP_2 and redistributes when PLC hydrolyzes PIP_2.[25] Under basal conditions,

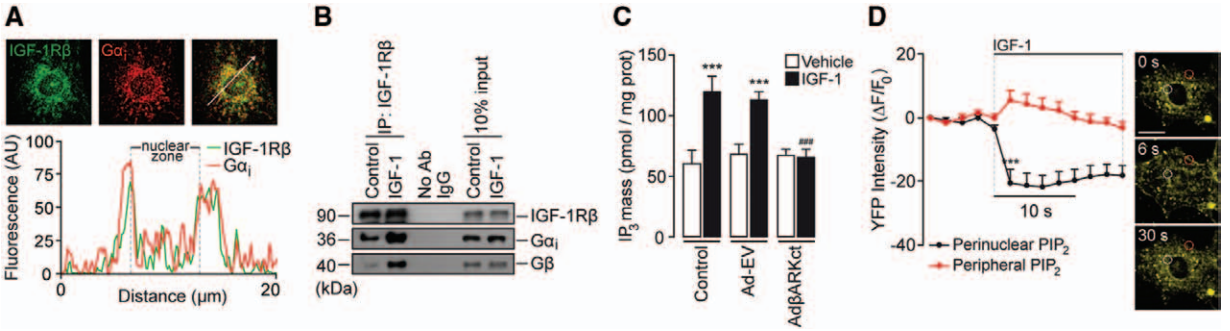

Figure 6. Perinuclear compartmentation of insulin-like growth factor 1 (IGF-1)–induced signaling. A, Images of single-plane confocal immunofluorescence performed against the β-subunit of IGF-1 receptor (IGF-1R) and $G\alpha_i$ protein on permeabilized cardiac myocytes; the **arrow** denotes a linear fluorescence profile analysis of colocalization, shown in the **bottom**. **B**, Immunoprecipitation (IP) was performed using antibodies against the IGF-1Rβ on total protein extracts from untreated neonatal cardiac myocytes (control) or treated with 10 nmol/L IGF-1 for 1 minute (IGF-1). Internal IP controls were performed using either no antibody (No Ab) or an isotype IgG. Western blot analysis was performed using antibodies against IGF-1Rβ, Gβ, or $G\alpha_i$ antibodies. Blots are representative of 3 independent experiments. **C,** Radioligand binding of intracellular inositol 1,4,5-trisphosphate (IP_3) levels in response to stimulation with IGF-1 (10 nmol/L, 30 seconds) or vehicle, using control cardiac myocytes (untransduced) or transduced with adenoviruses encoding a Gβγ-dimer inhibitory peptide (βARKct) or empty vector (EV), as indicated (n=6, statistical significance was calculated by 2-way ANOVA, ***P<0.001 vs vehicle, ###P<0.001 vs EV+IGF-1, values are expressed as mean±SEM). **D,** Dynamic imaging of phosphatidylinositol 4,5-biphosphate (PIP_2) cleavage in response to IGF-1 stimulation using a yellow fluorescent protein–based $PH_{PLC\delta}$ reporter; fluorescence was quantified in perinuclear vs peripheral zones as indicated (denoted by white and red circles, respectively, on the images); representative images are shown (n=6, statistical significance was calculated by *t* test, ***P<0.001 vs peripheral ROI, values are expressed as mean±SEM). PH indicates pleckstrin homology domain; and PLC, phospholipase C.

the probe displayed a perinuclear and peripheral distribution, but in response to IGF-1, fluorescence was rapidly lost exclusively in the perinuclear zones and not in peripheral regions, indicating perinuclear compartmentation of IP_3 production (Figure 6D). The Gα protein–sensitive PLCβ3 exhibited the same perinuclear localization as the IGF-1R (Online Figure VIIA), whereas the tyrosine kinase–sensitive and Gβγ-sensitive PLCγ displayed a peripheral pool and also a perinuclear pool (Online Figure VIIB). In response to IGF-1, a rapid rise in the fluorescence of phosphorylated PLCγ was detected in the perinuclear region, without significant changes in the phosphorylation of the more peripheral pool (Online Figure VIIC). This is consistent with the perinuclear localization of IGF-1R upstream to both PLC subtypes. We have previously reported that effects of IGF-1 are dependent on IP_3Rs.[11] We now addressed whether IP_3Rs are located in the nucleus. In agreement with previous reports,[9,11,26] we observed a nuclear distribution of IP_3Rs when using an antibody that recognizes all 3 isoforms (Online Figure VIID), as well as a more pronounced distribution of type-2 IP_3R (Online Figure VIIE). Type-2 IP_3R has been previously described in perinuclear T-tubule microdomains, in close contact with the nuclear envelope.[27] Altogether, the results from this study confirm that a complete system for the generation of IP_3-mediated signals is present in the perinuclear region of these cells and is able to respond to extracellular IGF-1 binding by activation of IGF-1R, a locally restricted hydrolysis of PIP_2, IP_3 production, nuclear Ca^{2+} release, and MEF2C activation.

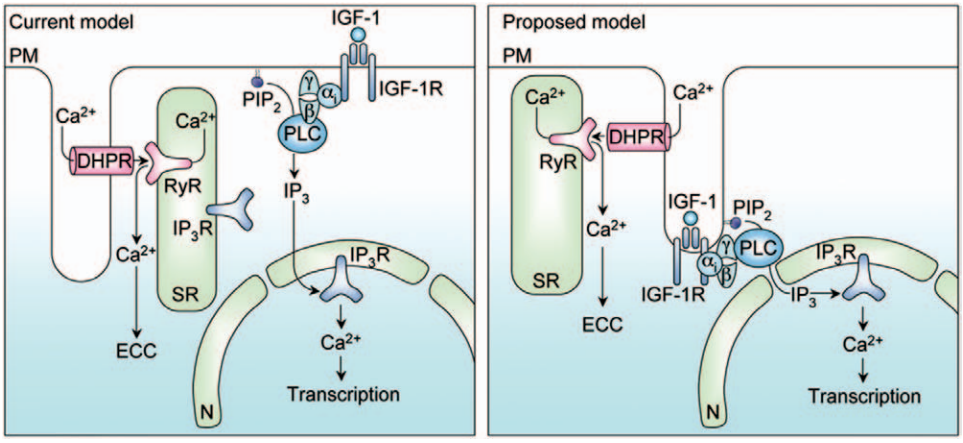

Figure 7. Working model. The current model that explains the functional separation of contractile vs signaling Ca^{2+} is based on the well-established compartmentation of excitation–contraction coupling (ECC) but not on compartmented inositol 1,4,5-trisphosphate (IP_3)–dependent pathways. In this model, IP_3 diffuses from the peripheral plasma membrane (PM) to the nucleus (N), bypassing IP_3 receptors (IP_3Rs) present in peripheral sarcoplasmic reticulum (SR). The proposed model situates the insulin-like growth factor 1 receptor (IGF-1R) signaling complex in plasma membrane invaginations of perinuclear localization, forming a microdomain where IP_3 is locally produced in response to extracellular stimulation, leading directly to nuclear Ca^{2+} signaling independently of ECC.

Discussion

Ca^{2+}-dependent gene expression is a widely described phenomenon in different cell types.[28,29] Despite numerous theories postulated to explain the versatility of roles played by intracellular Ca^{2+} signals,[9,30] the regulation of this process remains particularly difficult to understand in cardiac myocytes, where free Ca^{2+} levels are continually changing. Nuclear Ca^{2+} transients have been described in both skeletal and cardiac myocytes,[31,32] and the possibility of IP_3 being capable of releasing Ca^{2+} to the nucleoplasm from nuclear receptors has been explored.[31] The question has remained, however: how can the nuclear response occur before or in the absence of cytosolic activity (as observed in Figure 1). The existence of a specialized membrane structure, channeling the extracellular growth factor to a juxtanuclear receptor signaling complex, explains how nuclear-specific Ca^{2+} changes that modulate gene expression can be insulated from the large-amplitude changes in cytosolic Ca^{2+} that arise with every heart cell contraction (see our proposed model in Figure 7).

The results from our working model strongly suggest that nuclear Ca^{2+} can be independently regulated from cytosolic Ca^{2+}, thanks to a locally restricted signaling toolkit. The use of nuclear-targeted parvalbumin evidenced that the Ca^{2+} signal is generated in the nucleus and is fully independent of cytosolic Ca^{2+} release. In addition, using human embryonic cardiac myocytes, we observed that the cytosolic component precedes the nuclear component of the basal Ca^{2+} oscillations, indicating its primarily cytosolic origin. In contrast, the nuclear Ca^{2+} signal triggered by IGF-1 in these cells was—as in murine cells—originated in the nucleus, and then followed by the cytosolic component. Previous work with parvalbumins by Leite et al[33] demonstrated that spontaneous Ca^{2+} activity was more affected by buffering cytosolic Ca^{2+} than nuclear Ca^{2+}, which agrees with our view that there is a separate control of both Ca^{2+} toolkits. Recently, the same group showed that nuclear IP_3 buffering abrogated the effects of endothelin-1 and IGF-1 on cardiac hypertrophy.[34] Our work complements these observations, providing the mechanism by which IP_3 is able to exert nuclear effects in response to extracellular stimulation without an impact on cytosolic IP_3-mediated Ca^{2+} signaling or the need of the messenger IP_3 to diffuse from the peripheral cell surface. The ensemble of our experiments suggests that such control is achieved by the local compartmentation of the necessary elements to trigger Ca^{2+} release within perinuclear microdomains. In particular, our results suggest that although T-tubules are the platform tunneling an extracellular ligand in close proximity to the nucleus, it is the perinuclear localization of the IGF-1R complex in these structures that allows the space-restricted triggering of nuclear Ca^{2+} release without having a significant impact on cytosolic Ca^{2+}. In support of this concept, a separate distribution of sarcolemmal receptors in the surface of cardiac myocytes versus the interior of T-tubules has been observed previously.[35] In rodents, β2-adrenergic receptor–induced cAMP signals are locally restricted to deep T-tubules, whereas β1-adrenergic receptors are distributed across the entire sarcolemma, and this allows the separation and spatial confinement of their downstream effects.[35] The mechanism restricting the localization of the sarcolemmal receptors to the perinuclear region remains elusive, however, and is our current line of investigation.

Recently, it has been described by electron microscopy that T-tubules establish contacts with the nuclear envelope, forming perinuclear microdomains where type-2 IP_3Rs mediate nuclear Ca^{2+} signaling.[27] Importantly here, we have found that this Ca^{2+} signaling system is indeed activated in response to an extracellular ligand, and this involves the sequential and specific action of a perinuclear pool of sarcolemmal IGF-1R, heterotrimeric G protein, PLCγ/β3, localized IP_3 production, IP_3Rs, and MEF2C activation. Our findings, therefore, provide the functional basis for these signaling structures and also represent a novel signaling mechanism in cell biology. Organelle interactions with the nucleus or with the cell surface are well-known. However, the plasma membrane–nucleus contacts described here establish for the first time a direct bridge between extracellular stimulation and nuclear gene expression, through the controlled compartmentation of Ca^{2+} signaling.

We observed that the structure of cardiac myocytes, based on plasma membrane invaginations, provides a localized platform for the nuclear compartmentation of a surface receptor. It is known that neonatal cardiac myocytes do not have a well-developed T-tubule network, and accordingly we observed that in these cells T-tubules were less interconnected in comparison with our experiments with adult cardiac myocytes. However, our set of experiments with formamide for the disruption of T-tubules and with MβCD for the disruption of lipid rafts demonstrated that plasma membrane invaginations with mixed characteristics of lipid rafts and T-tubules do exist in neonatal cells and are essential for excitation–contraction coupling and for IGF-1R signaling to the nucleus. This is in agreement with previous observations indicating that both types of plasma membrane invaginations share the same biogenesis mechanisms.[22] We refer to these structures here as pre–T-tubules, and we speculate that the MEF2C-dependent genetic program activated by IGF-1R–mediated Ca^{2+} signaling contributes to the establishment of the more mature cardiac phenotype at this particular stage of differentiation. In a similar way, a distribution of the IGF-1R in lipid rafts/caveolae has been described as necessary for adipocyte differentiation,[23] and IGF-1 is indeed an essential factor regulating not only cardiac myocyte differentiation[36] but also hypertrophy in pathological models where embryonic gene programs are reactivated.[37] The role of T-tubules in nuclear signaling may also have important ramifications for disease states, such as heart disease or ischemia, when T-tubules are reduced, swollen, or otherwise dysfunctional.[38] The IGF-1R signaling pathways are known to promote cardiac growth, improve cardiac contractility, prevent cardiac myocyte apoptosis, and contribute to cardiac metabolic adaptability.[39–42]

In conclusion, the data presented here establish evidence in favor of the compartmentation of Ca^{2+} signals and provide the first functional basis of a novel form of interorganelle communication that directly links plasma membrane signaling to nuclear Ca^{2+}-dependent processes.

Acknowledgments

We are grateful to Dr Eva Wärdell and Dr Ulrika Felldin for their assistance in obtaining human embryonic cardiomyocytes. We also thank Dr Håkan Westerblad and Shi-jin Zhang for their assistance in obtaining adult rat cardiomyocytes. We thank Dr Carla Ortiz for help with

organization of the article, Göran Mansson for 3-dimensional imaging assistance, Sam Ranasinghe for assistance with microscopy facilities, as well as Fidel Albornoz and Johnny Söderlund for technical assistance.

Sources of Funding

This work was funded by Comision Nacional de Investigacion Cientifica y Tecnologica (CONICYT), Chile: Anillo ACT 1111 (to S.L., E.J., and A.F.G.Q.), Programa Fondo de Investigación Avanzado en Areas Prioritarias (FONDAP) 1501006 (to S.L., E.J., and A.F.G.Q.), by the Swedish Research Council (grant 2009–3364, 2010–4392, Center of Excellence in Developmental Biology for Regenerative Medicine [DBRM] to P.U.), and by Wallenberg (Center of Live Imaging of Cells Karolinska Institutet [CLICK] to P.U.). We also thank Becas Chile for the funding to J.M.V. and to Comision Nacional de Investigacion Cientifica y Tecnologica (CONICYT) Chile for the funding to C.I., J.P.M., and P.R.

Disclosures

None.

References

1. Gerasimenko O, Gerasimenko J. New aspects of nuclear calcium signalling. *J Cell Sci*. 2004;117:3087–3094.
2. Hardingham GE, Chawla S, Johnson CM, Bading H. Distinct functions of nuclear and cytoplasmic calcium in the control of gene expression. *Nature*. 1997;385:260–265.
3. Passier R, Zeng H, Frey N, Naya FJ, Nicol RL, McKinsey TA, Overbeek P, Richardson JA, Grant SR, Olson EN. CaM kinase signaling induces cardiac hypertrophy and activates the MEF2 transcription factor in vivo. *J Clin Invest*. 2000;105:1395–1406.
4. McKinsey TA, Zhang CL, Lu J, Olson EN. Signal-dependent nuclear export of a histone deacetylase regulates muscle differentiation. *Nature*. 2000;408:106–111.
5. Stehno-Bittel L, Perez-Terzic C, Clapham DE. Diffusion across the nuclear envelope inhibited by depletion of the nuclear Ca2+ store. *Science*. 1995;270:1835–1838.
6. Zhang SJ, Zou M, Lu L, Lau D, Ditzel DA, Delucinge-Vivier C, Aso Y, Descombes P, Bading H. Nuclear calcium signalling controls expression of a large gene pool: identification of a gene program for acquired neuroprotection induced by synaptic activity. *Plos Genet*. 2009;5:E1000604.
7. Lipp P, Thomas D, Berridge MJ, Bootman MD. Nuclear calcium signalling by individual cytoplasmic calcium puffs. *EMBO J*. 1997;16:7166–7173.
8. al-Mohanna FA, Caddy KW, Bolsover SR. The nucleus is insulated from large cytosolic calcium ion changes. *Nature*. 1994;367:745–750.
9. Wu X, Zhang T, Bossuyt J, Li X, McKinsey TA, Dedman JR, Olson EN, Chen J, Brown JH, Bers DM. Local InsP3-dependent perinuclear Ca2+ signaling in cardiac myocyte excitation-transcription coupling. *J Clin Invest*. 2006;116:675–682.
10. Leite MF, Thrower EC, Echevarria W, Koulen P, Hirata K, Bennett AM, Ehrlich BE, Nathanson MH. Nuclear and cytosolic calcium are regulated independently. *Proc Natl Acad Sci USA*. 2003;100:2975–2980.
11. Ibarra C, Estrada M, Carrasco L, Chiong M, Liberona JL, Cardenas C, Díaz-Araya G, Jaimovich E, Lavandero S. Insulin-like growth factor-1 induces an inositol 1,4,5-trisphosphate-dependent increase in nuclear and cytosolic calcium in cultured rat cardiac myocytes. *J Biol Chem*. 2004;279:7554–7565.
12. Echevarría W, Leite MF, Guerra MT, Zipfel WR, Nathanson MH. Regulation of calcium signals in the nucleus by a nucleoplasmic reticulum. *Nat Cell Biol*. 2003;5:440–446.
13. Bers DM. Cardiac excitation-contraction coupling. *Nature*. 2002;415:198–205.
14. Foncea R, Andersson M, Ketterman A, Blakesley V, Sapag-Hagar M, Sugden PH, LeRoith D, Lavandero S. Insulin-like growth factor-I rapidly activates multiple signal transduction pathways in cultured rat cardiac myocytes. *J Biol Chem*. 1997;272:19115–19124.
15. Andersson DC, Fauconnier J, Park CB, Zhang SJ, Thireau J, Ivarsson N, Larsson NG, Westerblad H. Enhanced cardiomyocyte Ca(2+) cycling precedes terminal AV-block in mitochondrial cardiomyopathy Mterf3 KO mice. *Antioxid Redox Signal*. 2011;15:2455–2464.
16. Sambrano GR, Fraser I, Han H, Ni Y, O'Connell T, Yan Z, Stull JT. Navigating the signalling network in mouse cardiac myocytes. *Nature*. 2002;420:712–714.
17. Zhou YY, Wang SQ, Zhu WZ, Chruscinski A, Kobilka BK, Ziman B, Wang S, Lakatta EG, Cheng H, Xiao RP. Culture and adenoviral infection of adult mouse cardiac myocytes: methods for cellular genetic physiology. *Am J Physiol Heart Circ Physiol*. 2000;279:H429–H436.
18. Obame FN, Plin-Mercier C, Assaly R, Zini R, Dubois-Randé JL, Berdeaux A, Morin D. Cardioprotective effect of morphine and a blocker of glycogen synthase kinase 3 beta, SB216763 [3-(2,4-dichlorophenyl)-4(1-methyl-1H-indol-3-yl)-1H-pyrrole-2,5-dione], via inhibition of the mitochondrial permeability transition pore. *J Pharmacol Exp Ther*. 2008;326:252–258.
19. Genead R, Danielsson C, Wärdell E, Kjaeldgaard A, Westgren M, Sundström E, Franco-Cereceda A, Sylvén C, Grinnemo KH. Early first trimester human embryonic cardiac Islet-1 progenitor cells and cardiomyocytes: Immunohistochemical and electrophysiological characterization. *Stem Cell Res*. 2010;4:69–76.
20. Estrada M, Uhlen P, Ehrlich BE. Ca2+ oscillations induced by testosterone enhance neurite outgrowth. *J Cell Sci*. 2006;119:733–743.
21. Brette F, Komukai K, Orchard CH. Validation of formamide as a detubulation agent in isolated rat cardiac cells. *Am J Physiol Heart Circ Physiol*. 2002;283:H1720–H1728.
22. Carozzi AJ, Ikonen E, Lindsay MR, Parton RG. Role of cholesterol in developing T-tubules: analogous mechanisms for T-tubule and caveolae biogenesis. *Traffic*. 2000;1:326–341.
23. Huo H, Guo X, Hong S, Jiang M, Liu X, Liao K. Lipid rafts/caveolae are essential for insulin-like growth factor-1 receptor signaling during 3T3-L1 preadipocyte differentiation induction. *J Biol Chem*. 2003;278:11561–11569.
24. Dalle S, Ricketts W, Imamura T, Vollenweider P, Olefsky JM. Insulin and insulin-like growth factor I receptors utilize different G protein signaling components. *J Biol Chem*. 2001;276:15688–15695.
25. Várnai P, Balla T. Live cell imaging of phosphoinositide dynamics with fluorescent protein domains. *Biochim Biophys Acta*. 2006;1761:957–967.
26. Luo D, Yang D, Lan X, Li K, Li X, Chen J, Zhang Y, Xiao RP, Han Q, Cheng H. Nuclear Ca2+ sparks and waves mediated by inositol 1,4,5-trisphosphate receptors in neonatal rat cardiomyocytes. *Cell Calcium*. 2008;43:165–174.
27. Escobar M, Cardenas C, Colavita K, Petrenko NB, Franzini-Armstrong C. Structural evidence for perinuclear calcium microdomains in cardiac myocytes. *J Mol Cell Cardiol*. 2011;50:451–459.
28. Berridge MJ, Bootman MD, Roderick HL. Calcium signalling: dynamics, homeostasis and remodelling. *Nat Rev Mol Cell Biol*. 2003;4:517–529.
29. Frey N, McKinsey TA, Olson EN. Decoding calcium signals involved in cardiac growth and function. *Nat Med*. 2000;6:1221–1227.
30. Goonasekera SA, Molkentin JD. Unraveling the secrets of a double life: contractile versus signaling Ca2+ in a cardiac myocyte. *J Mol Cell Cardiol*. 2012;52:317–322.
31. Cárdenas C, Liberona JL, Molgó J, Colasante C, Mignery GA, Jaimovich E. Nuclear inositol 1,4,5-trisphosphate receptors regulate local Ca2+ transients and modulate cAMP response element binding protein phosphorylation. *J Cell Sci*. 2005;118:3131–3140.
32. Zima AV, Bare DJ, Mignery GA, Blatter LA. IP3-dependent nuclear Ca2+ signalling in the mammalian heart. *J Physiol (Lond)*. 2007;584:601–611.
33. Guatimosim S, Amaya MJ, Guerra MT, Aguiar CJ, Goes AM, Gómez-Viquez NL, Rodrigues MA, Gomes DA, Martins-Cruz J, Lederer WJ, Leite MF. Nuclear Ca2+ regulates cardiomyocyte function. *Cell Calcium*. 2008;44:230–242.
34. Arantes LA, Aguiar CJ, Amaya MJ, Figueiró NC, Andrade LM, Rocha-Resende C, Resende RR, Franchini KG, Guatimosim S, Leite MF. Nuclear inositol 1,4,5-trisphosphate is a necessary and conserved signal for the induction of both pathological and physiological cardiomyocyte hypertrophy. *J Mol Cell Cardiol*. 2012;53:475–486.
35. Nikolaev VO, Moshkov A, Lyon AR, Miragoli M, Novak P, Paur H, Lohse MJ, Korchev YE, Harding SE, Gorelik J. Beta2-adrenergic receptor redistribution in heart failure changes cAMP compartmentation. *Science*. 2010;327:1653–1657.
36. Laustsen PG, Russell SJ, Cui L, Entingh-Pearsall A, Holzenberger M, Liao R, Kahn CR. Essential role of insulin and insulin-like growth factor 1 receptor signaling in cardiac development and function. *Mol Cell Biol*. 2007;27:1649–1664.
37. Muñoz JP, Collao A, Chiong M, Maldonado C, Adasme T, Carrasco L, Ocaranza P, Bravo R, Gonzalez L, Díaz-Araya G, Hidalgo C, Lavandero S. The transcription factor MEF2C mediates cardiomyocyte hypertrophy induced by IGF-1 signaling. *Biochem Biophys Res Commun*. 2009;388:155–160.

38. Lyon AR, MacLeod KT, Zhang Y, Garcia E, Kanda GK, Lab MJ, Korchev YE, Harding SE, Gorelik J. Loss of T-tubules and other changes to surface topography in ventricular myocytes from failing human and rat heart. *Proc Natl Acad Sci USA*. 2009;106:6854–6859.
39. Anversa P. Aging and longevity: the IGF-1 enigma. *Circ Res*. 2005;97:411–414.
40. Ebensperger R, Acevedo E, Meléndez J, Corbalán R, Acevedo M, Sapag-Hagar M, Jalil JE, Lavandero S. Selective increase in cardiac IGF-1 in a rat model of ventricular hypertrophy. *Biochem Biophys Res Commun*. 1998;243:20–24.
41. Ren J, Samson WK, Sowers JR. Insulin-like growth factor I as a cardiac hormone: physiological and pathophysiological implications in heart disease. *J Mol Cell Cardiol*. 1999;31:2049–2061.
42. Troncoso R, Vicencio JM, Parra V, et al. Energy-preserving effects of IGF-1 antagonize starvation-induced cardiac autophagy. *Cardiovasc Res*. 2012;93:320–329.

Novelty and Significance

What Is Known?

- Cytosolic calcium signaling is essential for cardiomyocyte contraction.
- Changes in calcium levels in the nucleus regulate gene expression, but the mechanisms regulating nuclear calcium are unclear.
- The extracellular growth factor insulin-like growth factor 1 activates a calcium-dependent gene program in cardiac cells.
- Neonatal cardiac myocytes do not contain T-tubules.

What New Information Does This Article Contribute?

- In response to extracellular stimulation, nuclear calcium can be regulated independently of cytosolic calcium as a result of the compartmentation of its release.
- The insulin-like growth factor 1 receptor is located in perinuclear invaginations of the plasma membrane, triggering nuclear calcium release locally.
- Neonatal cardiac myocytes contain pre–T-tubules with mixed characteristics of T-tubules and lipid rafts, which are essential for contraction and nuclear calcium signals.

Electric excitation is essential for every heartbeat. A single electric impulse triggers contraction as a result of a transient increase in cytosolic calcium levels in cardiac myocytes. However, in these cells calcium in the nucleus regulates gene expression. How nuclear calcium signals are achieved independently of cytosolic calcium is not clear. The insulin-like growth factor 1 receptor is known to activate gene programs during cardiac development and pathology, and its location in T-tubules is essential for such function. We found that insulin-like growth factor 1 can trigger a nuclear calcium signal in embryonic, neonatal, or adult cardiomyocytes, without involving cytosolic calcium. This is achieved by the activation of plasma membrane receptors localized to sarcolemmal invaginations resembling T-tubules that extend deep within the cell as far as the nucleus. Although neonatal cardiac myocytes are believed to lack T-tubules, we observed that these do contain plasma membrane invaginations that are essential for nuclear calcium signals and which we call pre–T-tubules. This study provides new insight into the regulation of calcium signaling in cardiomyocytes by identifying highly compartmentalized localization of signaling complexes in plasma membrane invaginations adjacent to the nucleus.

Online Figure I

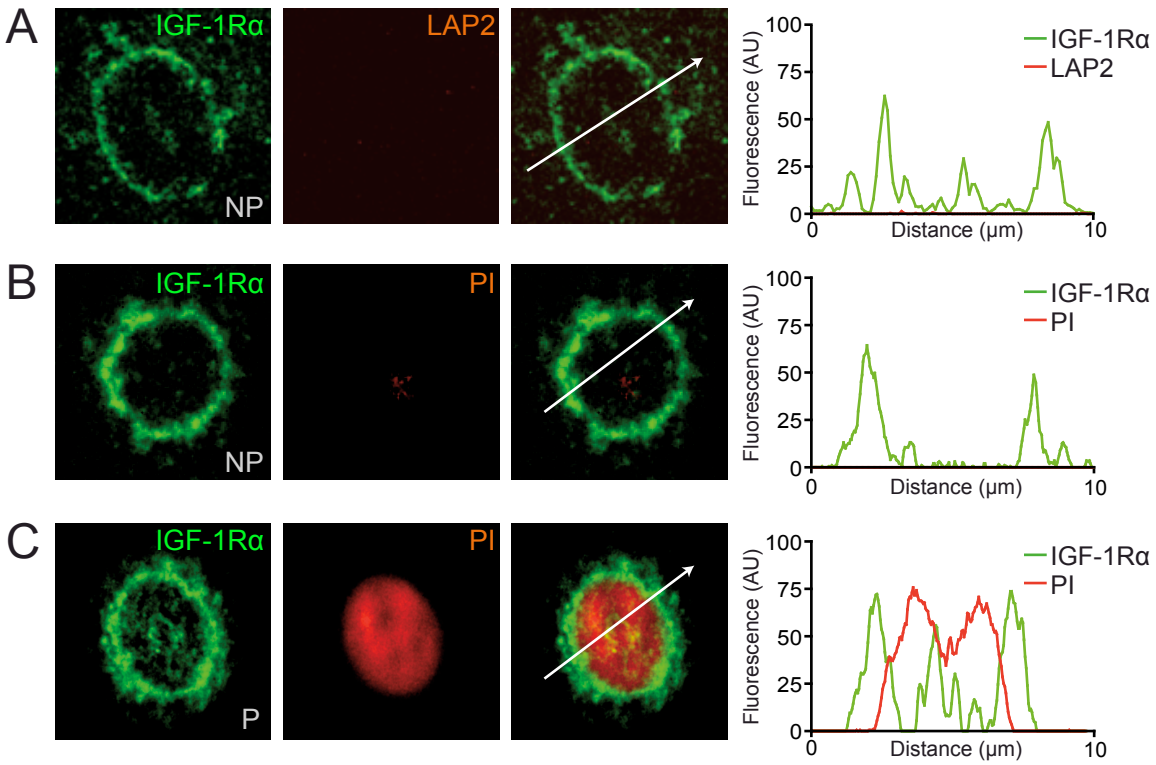

Online Figure I. Absence of intracellular staining in non-permeabilized neonatal cardiac myocytes. **(A)** Single-plane confocal images of non-permeabilized (NP) fixed cardiac myocytes immunostained with antibodies against an extracellular epitope of IGF-1Rα and the nuclear lamina-associated protein LAP2; A linear fluorescence profile analysis of co-localization is shown in the right panel. **(B)** Single-plane confocal images of NP fixed cardiac myocytes immunostained with an antibody against an extracellular epitope of IGF-1Rα and counterstained with propidium iodide (PI); a linear fluorescence profile analysis is shown. **(C)** Single-plane confocal images of fixed and permeabilized (P) cardiac myocytes immunostained with an antibody against an extracellular epitope of IGF-1Rα and counterstained with propidium iodide (PI); a linear fluorescence profile analysis of co-localization is shown.

Online Figure II

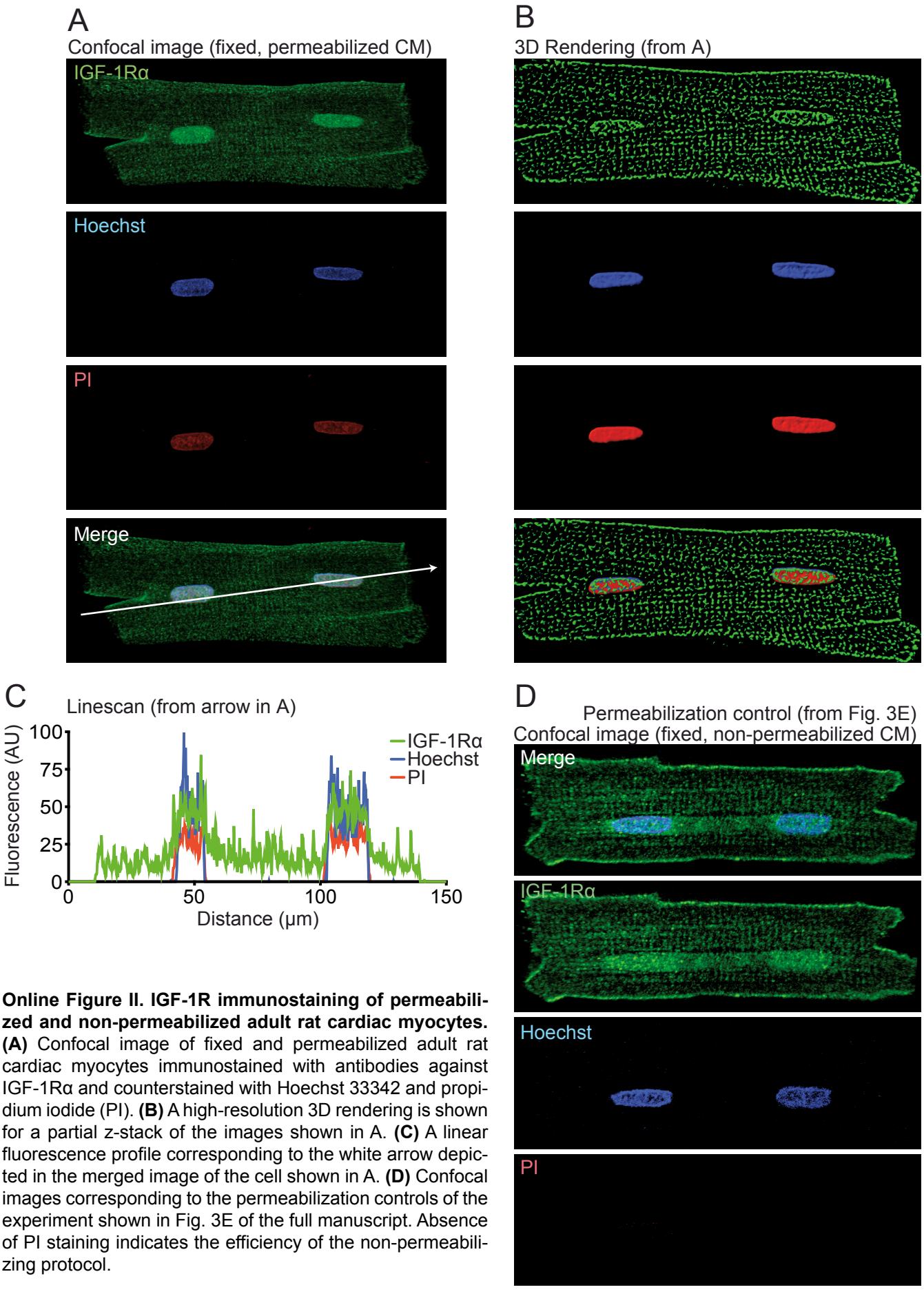

Online Figure II. IGF-1R immunostaining of permeabilized and non-permeabilized adult rat cardiac myocytes. **(A)** Confocal image of fixed and permeabilized adult rat cardiac myocytes immunostained with antibodies against IGF-1Rα and counterstained with Hoechst 33342 and propidium iodide (PI). **(B)** A high-resolution 3D rendering is shown for a partial z-stack of the images shown in A. **(C)** A linear fluorescence profile corresponding to the white arrow depicted in the merged image of the cell shown in A. **(D)** Confocal images corresponding to the permeabilization controls of the experiment shown in Fig. 3E of the full manuscript. Absence of PI staining indicates the efficiency of the non-permeabilizing protocol.

Online Figure III

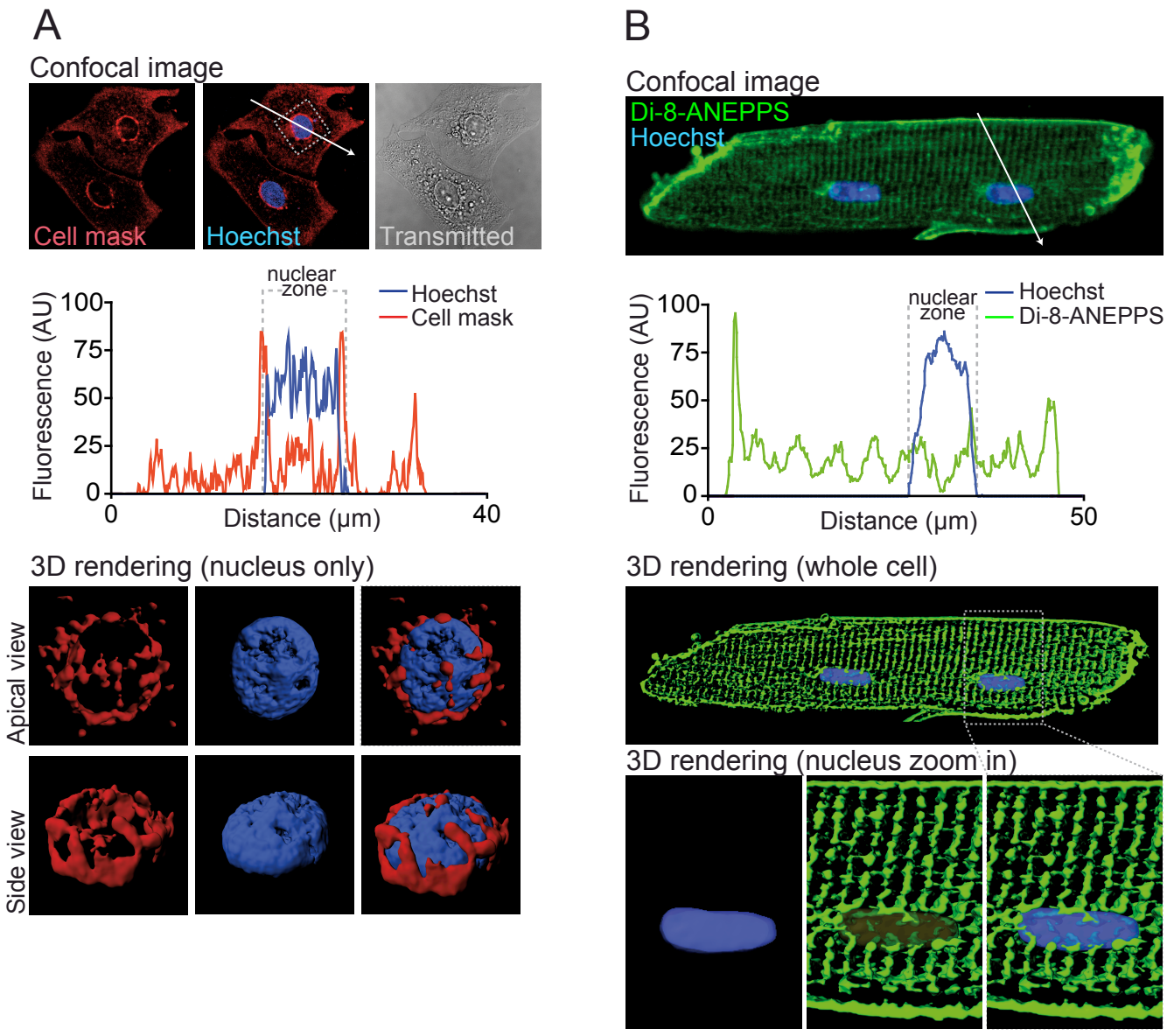

Online Figure III. Perinuclear plasma membrane invaginations. (A) Confocal stack images of live neonatal cardiac myocytes stained with Hoechst 33342 for 15 min and the plasma membrane stain Cell mask for 5 min before imaging (upper panel); the arrow denotes a linear fluorescence profile analysis, shown in the middle panel; the dotted box denotes the region used for a high resolution 3D rendering, shown in the bottom panel at different angles of view. **(B)** Confocal stack images of live adult mouse cardiac myocyte stained with Hoechst 33342 for 15 min and the plasma membrane stain Di-8-ANEPPS for 10 min before imaging (upper panel); the arrow denotes a linear fluorescence profile analysis, shown in the middle panel; a high resolution 3D rendering is shown on the lower panel (whole cell) and the dotted box denotes magnified views of the nucleus (lower panel). Data are representative of 6 independent experiments.

Online Figure IV

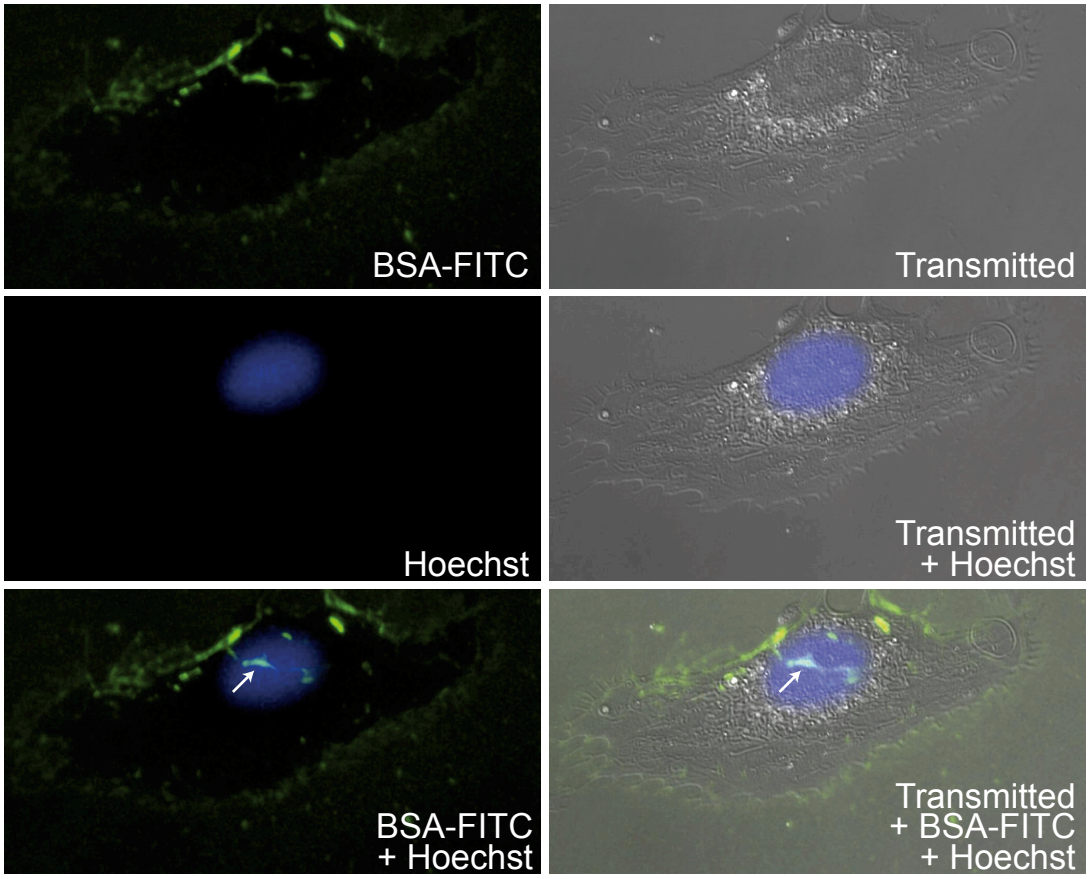

Online Figure IV. Staining of perinuclear sarcolemmal invaginations. Live cardiac myocytes from neonatal rats were stained with Hoechst 33342 and cell-impermeant albumin bound to FITC (BSA-FITC; 0,1%) for 3 min at room temperature. Single-plane confocal images of the FITC, UV and transmitted light channels are shown as indicated. White arrows denote zones where extracellular BSA-FITC is observed in tunnels through the nucleus.

Online Figure V

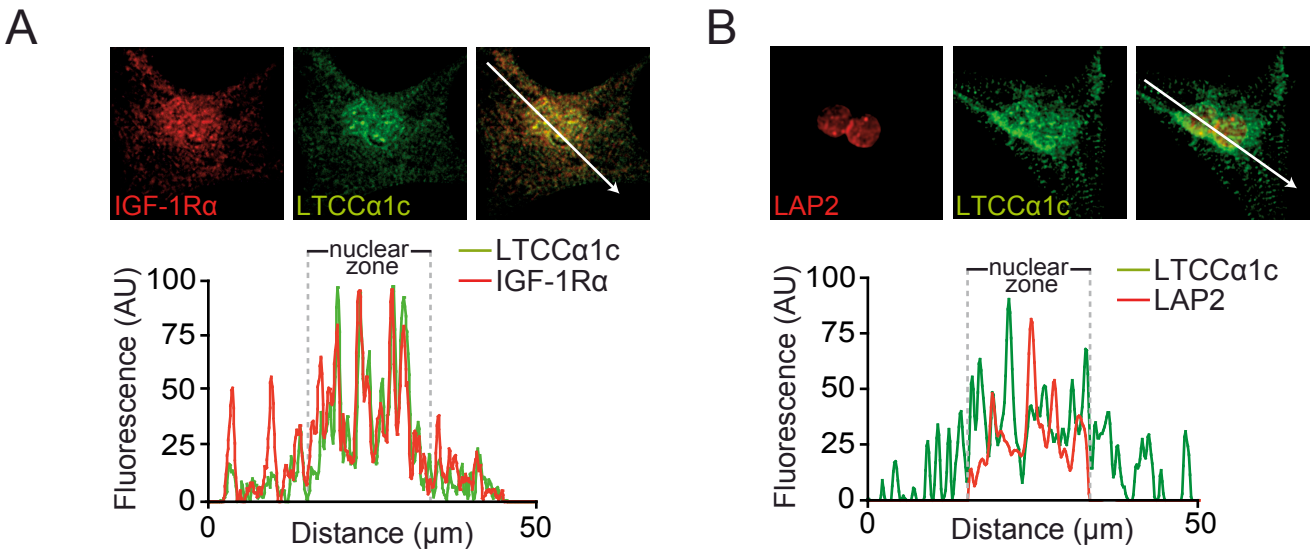

Online Figure V. Co-localization of IGF-1R, LAP2 and the α1c subunit of L-type Ca^{2+} channels. (A) Single-plane confocal images of immunofluorescence performed against the α1c subunit of L-type Ca^{2+} channels (LTCCα1c) and the α subunit of the IGF-1R; the arrow denotes a linear fluorescence profile analysis of co-localization, shown in the lower panel. **(B)** Images of single-plane confocal immunofluorescence performed against LTCCα1c and the nuclear lamina-associated protein LAP2; the arrow denotes a linear fluorescence profile analysis of co-localization, shown in the lower panel. Images are representative of 3 independent experiments.

Online Figure VI

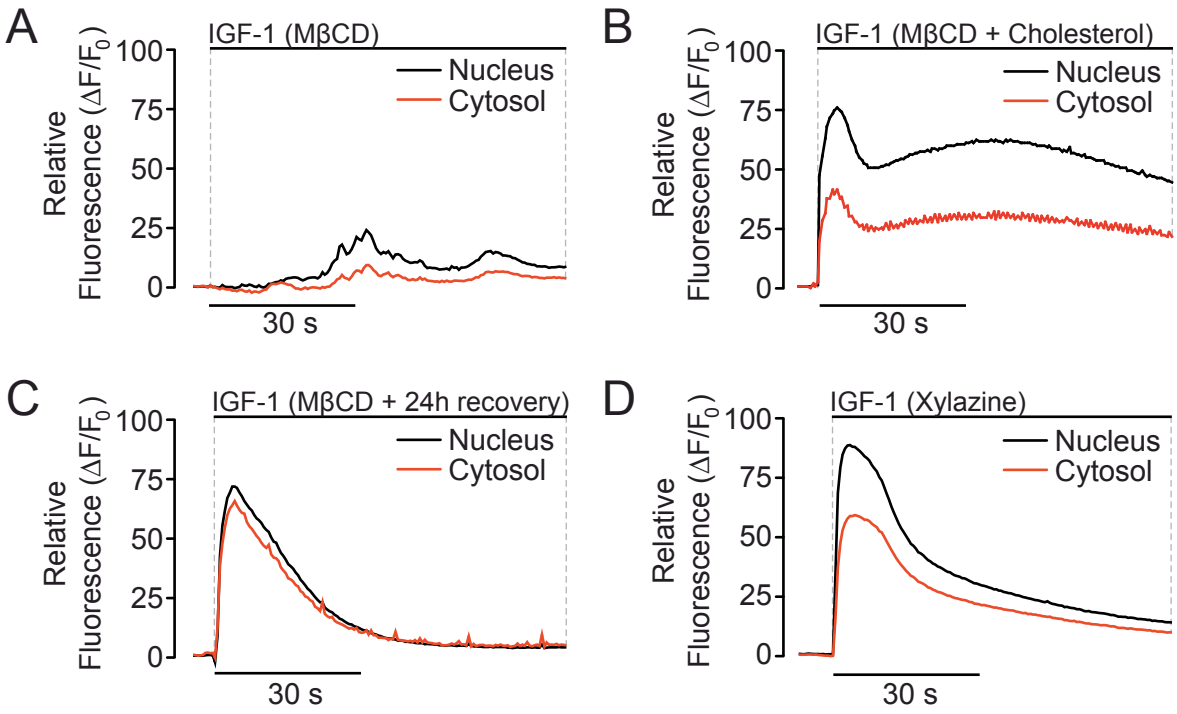

Online Figure VI. Disruption of lipid rafts abrogates the effects of IGF-1 on nuclear Ca^{2+}. (A) Ca^{2+} measurements were performed on cardiac myocytes subjected to acute disruption of lipid rafts by treatment with the cholesterol-binding agent methyl β cyclodextrin (MβCD) for 30 min and then stimulated with IGF-1; representative relative fluorescence values of nuclear vs. cytosolic regions are shown **(B)** Ca^{2+} measurements were performed on cardiac myocytes subjected to 30 min treatment with MβCD pre-complexed with 10 mM cholesterol for its inactivation, and then imaged and stimulated with IGF-1; representative relative fluorescence values of nuclear vs. cytosolic regions are shown **(C)** Ca^{2+} measurements were performed on cardiac myocytes subjected to acute disruption of lipid rafts with MβCD for 30 min and left to recover for 24 h before loading with fluo-3AM and stimulation with 10 nM IGF-1 for Ca^{2+} imaging; representative relative fluorescence values of nuclear vs. cytosolic regions are shown **(D)** Ca^{2+} measurements were performed on cardiac myocytes subjected to acute treatment with the unspecific lipid-binding reagent xylazine for 30 min prior to imaging and stimulation with IGF-1; representative relative fluorescence values of nuclear vs. cytosolic regions are shown.

Online Figure VII

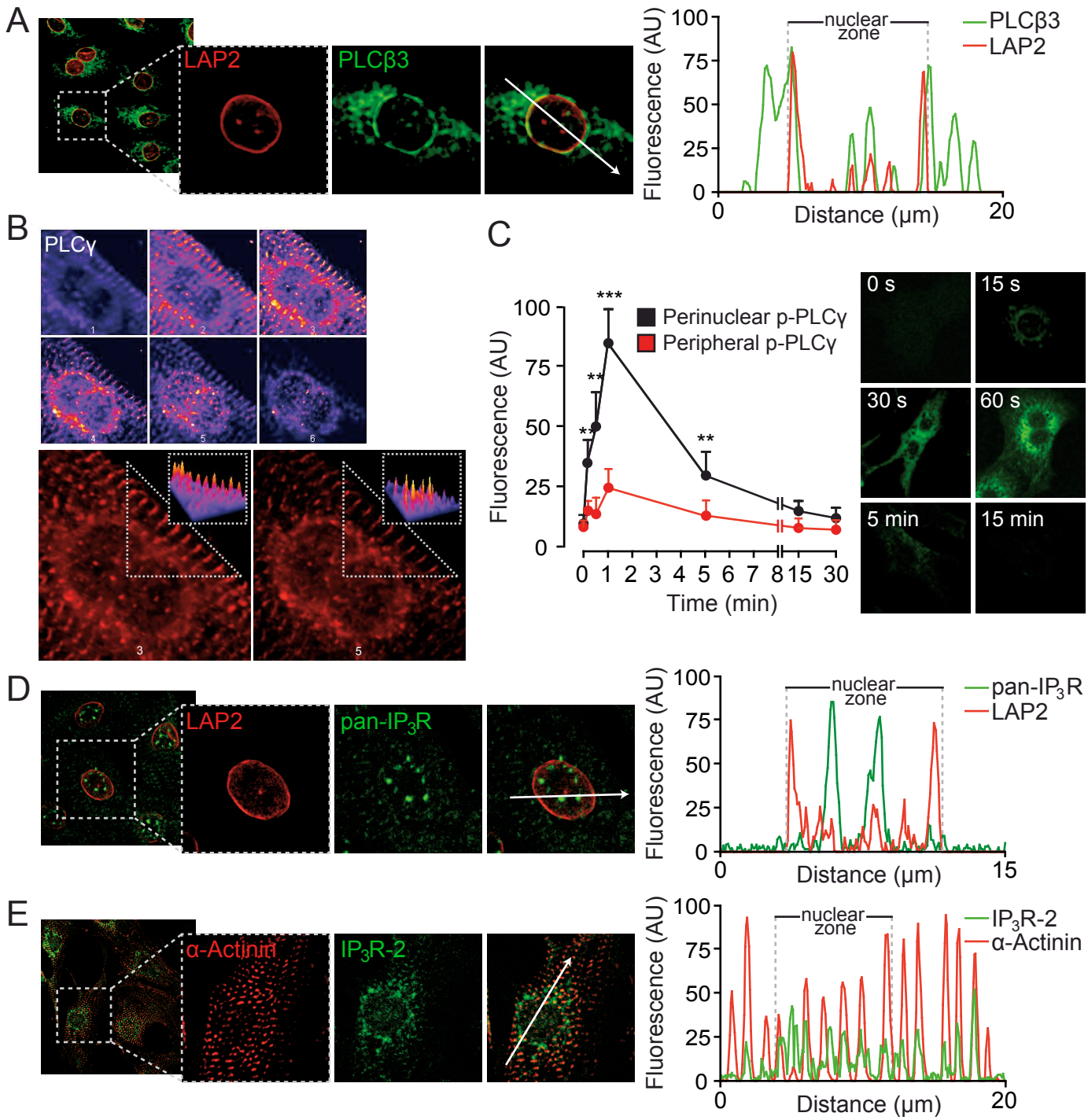

Online Figure VII. Perinuclear compartmentation of IGF-1-induced signalling to PLC and IP_3Rs. (A) Single-plane confocal images of immunofluorescence performed with antibodies against PLCβ3 and LAP2 on permeabilized cardiac myocytes; the arrow denotes a linear fluorescence profile analysis of co-localization, shown in the right panel. **(B)** Array of different confocal-plane images of immunofluorescence preformed against PLCγ in permeabilized cardiac myocytes, shown in pseudocolor (firescale, left panel) and in original color (Alexa-568, right panel); the dotted triangles denote the regions used for a surface-plot of the peripheral (picture 3) and perinuclear (picture 5) pools of PLCγ (lower panel, inset pictures). Images are representative of 3 independent experiments. **(C)** Immunofluorescence analysis of phosphorylated PLCγ in permeabilized cardiac myocytes stimulated with IGF-1 for the indicated time periods; the perinuclear vs. peripheral fluorescence intensity was quantified; representative images are shown (n = 6, statistical significance was calculated by t-test, ***P<0.001 and **P<0.01 vs. peripheral ROI, values are expressed as mean ± s.e.m.). **(D)** Single-plane confocal images of immunofluorescence against LAP2 and all-three IP_3R isoforms performed on permeabilized neonatal cardiac myocytes; a linear fluorescence profile analysis is shown. **(E)** Single-plane confocal images of immunofluorescence against α-actinin/IP_3R-2 on permeabilized cells and linear fluorescence profile analysis of co-localization. n = 6 for D and E.

2. Legends to Online Movies

Online Movie I. This movie shows the fast nuclear Ca^{2+} increase in response to IGF-1 stimulation in neonatal rat cardiac myocytes. Imaging was performed every 2 s over a period of 2 min. A firescale look-up-table was applied to the image sequence using the software ImageJ (QuickTime; 2.1 MB).

Online Movie II. This movie shows the nuclear zone of a non-permeabilized fixed cardiac myocyte immunostained with antibodies against IGF-1Rα (green) and Hoechst 33342 (blue). 3D rendering was performed using Imaris (QuickTime; 368 KB).

Online Movie III. This movie shows the nuclear zone of a living cardiac myocyte expressing IGF-1R-GFP (green) and stained with Hoechst 33342 (blue). 3D rendering was performed using Imaris (QuickTime; 1.3 MB).

Online Movie IV. This movie shows a living cardiac myocyte expressing IGF-1R-GFP (green), in which sarcolemma was stained with Cell Mask (red) and the nucleus with Hoechst 33342 (blue). 3D rendering was performed on a fraction of the cell to show perinuclear and intranuclear IGF-1R and sarcolemmal structures (QuickTime; 1.5 MB).

3. Full Materials and Methods

Primary culture of cardiac myocytes: Neonatal rat cardiac myocytes were prepared from hearts of 1-3 day old Sprague-Dawley rats as described [1]. Rats were bred in the animal facilities of the Faculty of Chemical and Pharmaceutical Sciences, University of Chile, conforming to the "Guide for the care and use of laboratory animals" (NIH publication No. 85-23, revised 1985). Ventricles were trisected, pooled and enzymatically digested in collagenase and pancreatin. After a pre-plating purification step, cells were plated for 16-18 h in a solution of Dulbecco's modified Eagle's medium (DMEM) and medium 199 (M199) in a volume proportion of 4:1, containing 10% (v/v) horse serum, 5% (v/v) heated-inactivated fetal calf serum, BrdU 100 mM and penicillin/streptomycin (100 units/ml). Cells were plated at a final density of 1-8 × 10^3/mm^2 on gelatin-coated culture plates or coverslips. Serum was withdrawn 24 h before all treatments.

Adult rat cardiac myocytes were prepared from adult Sprague-dawley rats using a procedure adapted from the protocol developed by the Alliance for Cellular Signalling (AfCS Procedure Protocol ID PP00000 125) [2]. Cardiac myocytes were placed on laminin-coated coverslips and allowed to attach for 20 mins before the start of experiments. Cells were maintained in Ca^{2+}-containing Krebs solution and used within the following 4 hours. Measurements were performed only in road-shape cells, as previously indicated [3].

Adult mouse cardiac myocytes were isolated using an adapted protocol from several studies [2, 4, 5]. Briefly, 10-12 weeks old C57BL6/J mice were heparinized (50 USP units) and anesthetized with a mixture of ketamine (140 mg/kg), xylazine (33 mg/kg) and atropine (9 mg/kg). Once pedal reflexes were inhibited, heart was rapidly removed, cannulated through the aorta and retrogradely perfused (3 ml/min) for 5 minutes at room temperature with Ca^{2+}-free perfusion buffer [NaCl 113 mM; KCl 4.7 mM; KH_2PO_4 0.6 mM; Na_2HPO_4 0.6 mM; $MgSO_4$-7H2O 1.2 mM; $NaHCO_3$ 12 mM; $KHCO_3$ 10 mM; Phenol Red 30 µM; HEPES-Na Salt 0.922 mM; Taurine 30 mM; Glucose 5.5 mM; 2,3-butanedione-monoxime 10 mM, pH 7.4] on a Langendorff perfusion apparatus. Enzymatic digestion was performed with digestion-Buffer [perfusion-buffer with LiberaseTM 0.2 mg/ml, Trypsin 2.5% 5.5 mM, DNase $5x10^{-3}$ U/ml and $CaCl_2$ 12.5 µM] for 20 minutes at 37 °C. When fully digested, both ventricles were isolated and softly disaggregated in 5 ml of digestion buffer. The resulting tissue-cell suspension was filtered through a 100 µm sterile mesh (SEFAR-Nitex) and transferred for enzymatic inactivation to a tube with 10 ml of stopping-buffer-1 [perfusion-buffer with 10% v/v FBS and $CaCl_2$ 12.5 µM]. After gravity sedimentation for 20 minutes, cardiac myocytes were resuspended in stopping-buffer-2 containing lower FBS concentration (5% v/v) for another 20 minutes. Ca^{2+}-reintroduction was performed in stopping-buffer-2 with five progressive increases in $CaCl_2$ concentrations (62 µM, 112 µM, 212 µM, 500 µM and 1 mM). Cells were resuspended and allowed to decant for 10 minutes in each step contributing to the cardiac myocyte suspension purification. The homogeneous rod-shaped cardiac myocyte suspension was then resuspended in M199 supplemented with Earle's salt solution and L-glutamine, Pen-Strep (1%), Creatine 5 mM, Taurine 5 mM, Carnitine 2 mM, BSA 2 g/l, blebbistatin 25 µM and FBS 5%. Plating was performed on 22 mm glass coverslips precoated with 200 µL of mouse Laminin 10 mg/ml in phosphate-buffered saline for 2h. After 1 hour in the 5% CO_2 incubator, serum-containing plating media was switched to Ca^{2+}-free hepes-buffered Krebs saline for microscopy imaging.

To collect human embryonic tissue, individual permission was obtained using a standard informed consent procedure. The Ethical Committee of the Karolinska University Hospital approved the use of tissues from surgically aborted human material. The abortion was preformed according to the techniques described in detail [6]. The investigation conforms to the principles outlined in the Declaration of Helsinki. To prepare cultured human embryonic cardiac myocytes, we followed a previously described protocol [7]. Briefly, aborted tissue (gestational week 8,5) was transported directly from the operating room to the dissection room. Time between abortion and culture preparation was 0.5-1 h. For culture, cardiac tissue was minced and incubated over night at 4 °C in Trypsin 0.5 mg/ml in HBSS supplemented with Ca and Mg. Next, the pre-treated heart pieces were digested in collagenase solution (Collagenase type 2, CLS-2 Worthington 160 U/mL in HBSS and supplemented with Ca and Mg) during continuous stirring at 37 °C in an incubator at humidified atmosphere containing 5% CO_2. The supernatant was saved every 15 min until all pieces were completely digested. The obtained cell suspension was washed by centrifugation at 140 *g* for 5 min and resuspended in knock-out Dulbecco's modified Eagle's medium (knock-out DMEM; Invitrogen, UK), nonessential amino acids (GTF, Sweden), Primocin 100 µg/mL medium (Amaxa Inc., USA), 0.1 mM β-mercaptoethanol (Invitrogen), glutamine 2 mM (Invitrogen), and insulin-transferrin-selenium supplement (Invitrogen). The cells were seeded directly onto plastic plates (Techno Plastic Products AG, Switzerland) in DMEM-Low Glucose Glutamax (Invitrogen, UK) supplemented with 10% fetal calf serum and MycoZap 5mM (Lonza, Switzerland) and cultured at 37 °C in a humidified atmosphere containing 5% CO_2, and the medium was changed twice weekly.

Adenovirus and cell transfection: Adenoviral vectors were propagated and purified as described [8]. Two transgenes were used: βARKct (Ad-βARKct, a gift from Dr. W. J. Koch, Duke University Medical Center, Durham, NC) [9] and an empty viral construct (Ad-EV). Cells were transduced at a MOI 300, with 95% transduction efficiency. For plasmid vectors, cells were transfected with 2 µg of: nuclear-exclusion signal parvalbumin (PV-NES); nuclear-localizing signal parvalbumin (PV-NLS) [10]; insulin-like growth factor type-1 receptor-GFP (IGF-1R-GFP); PLCδ-pleckstrin-homology domain-YFP (YFP-$PH_{PLC\delta}$, a gift from Dr. Tamas Balla, NIH, Bethesda, MD) [11], or a mixture of 1 µg of a MEF2C-luciferase reporter plasmid (a gift from Dr. J. D. Molkentin, Howard Hughes Medical Institute, Cincinnati, OH) plus 1 µg of PV-NES or PV-NLS, using Lipofectamin 2000 (Invitrogen). Plasmid-treated cells were incubated for 24 h before being used for experiments.

Luciferase enzymatic assay: Cells transiently expressing MEF2C-luciferase reporter and PV-NES or PV-NLS were stimulated with 10 nM IGF-1 for 24 h, and then lysed using passive lysis buffer (PLB, Promega). 20 µg of protein extract were used for a Luciferase/Renilla dual assay (Promega). Light emission was measured with a luminometer (GloMax, Promega) and expressed as Luciferase/Renilla relative light units over 10 s.

Dynamic Ca^{2+} imaging: Images were obtained using an inverted confocal microscope (Carl Zeiss Axiovert 135 M-LSM Microsystems) or a fluorescence microscope (Olympus Diaphot- TMD, Nikon Corporation). Cardiac myocytes were washed three times with Ca^{2+}-containing Krebs recording medium (KRB: 145 mM NaCl, 5 mM KCl, 2.6 mM $CaCl_2$, 1 mM $MgCl_2$, 10 mM HEPES-Na, 5.6 mM glucose, pH 7.4) and loaded with 5.4 µM fluo-3AM (coming from a stock in 20% pluronic acid in DMSO) for 20 min at 37 °C. After loading, cells were washed either with the same buffer or with a Ca^{2+}-free recording medium (Ca^{2+}-free KRB: 145 mM NaCl, 5 mM KCl, 1.0 mM EGTA, 1 mM $MgCl_2$, 10 mM HEPES-Na, 5.6 mM glucose, pH 7.4) and used for Ca^{2+} imaging within the next 2 h. Coverslips were mounted in 1 ml capacity chambers and placed in the microscope for fluorescence measurements after excitation with a 488-nm wavelength argon laser beam or filter system. IGF-1 was added directly in the chamber. The fluorescence images were collected every 0.4-2.0 s using an objective lens PlanApo 60X (numerical aperture 1.4). Image sequences were analyzed using the NIH open-access software ImageJ. Intracellular Ca^{2+} levels are expressed as the percentage of fluorescence intensity relative to basal fluorescence (a value stable for at least 3 min in resting conditions).

Immunofluorescence and co-localization analysis: For experiments using non-permeabilized cells, cells on glass coverslips were fixed with ice-cold PBS containing 2% paraformaldehyde for 15 min on ice and washed three times with ice-cold PBS. For experiments using permeabilized cells, cardiac myocytes were fixed as described above and then permeabilized with 0.3% Triton X-100 for 10 min on ice, followed by washing three times with ice-cold PBS. Nonspecific binding sites were blocked for 1 h with 5% BSA in PBS at room temperature. Cells were then incubated overnight at 4 °C with the following primary antibodies: IGF-1Rα (Santa Cruz Biotechnology, rabbit polyclonal 1:100), IGF-1Rβ (Santa Cruz Biotechnology, rabbit polyclonal 1:100, PLC-β3 (Santa Cruz Biotechnology, rabbit polyclonal 1:100), PLC-γ1/2 (BD biosciences, mouse monoclonal 1:50), pPLCγ (Santa Cruz Biotechnology, rabbit polyclonal 1:100), caveolin-3 (BD biosciences, mouse monoclonal 1:400), α1c-DHPR (Santa Cruz Biotechnology, rabbit polyclonal 1:100), $G\alpha_i$ (Santa Cruz Biotechnology, rabbit polyclonal 1:50), Gβ (Santa Cruz Biotechnology, rabbit polyclonal 1:50), α-actinin (BD Biosciences, mouse monoclonal 1:400), LAP-2 (BD Biosciences, mouse monoclonal 1:400), IP_3R type II (Santa Cruz Biotechnology, goat polyclonal 1:100) and pan-IP_3R (mouse monoclonal 1:400, a gift from Dr. B. Ehrlich, Yale University, New Haven, NY). Cardiac myocytes were washed three times with PBS and incubated for 1 h at room temperature with anti-rabbit, anti-mouse or anti-goat IgG-Alexa488 or IgG-Alexa556 secondary antibodies (Invitrogen). Control staining without primary and/or secondary antibodies was carried out systematically. Coverslips were mounted in Dako fluorescent mounting medium (DakoCytomation). Confocal fluorescent images were acquired in scanning confocal microscopes (Zeiss Axiovert 135, Zeiss LSM 510 Meta or a Zeiss LSM 700, Carl Zeiss Microsystems) and analyzed off-line using ImageJ software (NIH). Ten cycles of iterative deconvolution were applied to each image using experimental point-spread function, previously determined using 0.175 mm diameter-fluorescent control beads (invitrogen). Co-localization between independent fluorescent signals was determined by a linear fluorescence intensity profile analysis of each single fluorochrome, in indicated regions of interest using ImageJ software (NIH).

Plasma membrane and BSA-FITC staining in living cells: For the staining of sarcolemma, we used Cell Mask Orange plasma membrane stain (Invitrogen) according to the manufacturer's protocol. Briefly, cardiac myocytes grown on glass coverslips were stained for 5 min in 1 ml of a 2.5 μg/ml Cell Mask dilution in Ca^{2+} containing Krebs medium, cells were then washed three times in Ca^{2+}-free Krebs medium and immediately analyzed with a confocal microscope. For the staining of extracellular invaginations, cardiac myocytes grown on glass coverslips were washed three times with Ca^{2+}-free Krebs medium and then incubated with a 0.1% dilution of the cell-impermeant albumin covalently bound to FITC (BSA-FITC, Sigma-Aldrich) and Hoechst 33342 in Krebs medium for 3 min at room temperature. Cells were then washed three times with Ca^{2+}-free Krebs medium and fluorescence was analyzed immediately with a confocal microscope (Carl Zeiss Axiovert 135 M-LSM Microsystems).

3D rendering of images: For the 3D digital analysis of images, we used the software Imaris (Bitplane AG, Zurich). Rendering algorithms were applied with the software using stacks of deconvolved confocal images of 0.1 μm-thickness obtained with a Zeiss LSM 700 confocal microscope (Carl Zeiss Microsystems). Images were 3D cropped, 3D volumes were created for each channel independently using a single contrast correction algorithm. The diameter of the object-fitting sphere in the raw volume was 0.3 μm and the 3D surface area detail level was set to 0.2 μm. Local background subtraction method was used to set local contrast for each channel. Threshold and number of voxels for a given 3D surface were set accordingly to the minimum and maximum fluorescence intensities of the respective confocal Z-stack. Analyses were performed using fixed or living cardiac myocytes as indicated on each figure.

Subcellular fractions, immunoprecipitation and Western blotting: Subcellular fractions were obtained using Qproteome Cell Compartment Kit (Qiagen) according to the manufacturer's protocol. Equal amounts of cytosolic, membrane, and nuclear proteins were solubilized in NuPAGE LDS sample buffer (Invitrogen) and separated on NuPAGE denaturing bis-tris SDS-polyacrylamide gels (Invitrogen). Proteins were electrotransferred into nitrocellulose membranes (Hybon-C-Super, Amersham) and IGF-1R

subunits were detected using specific antibodies (anti-IGF-1Rβ, Cell Signaling, rabbit polyclonal 1:1000; anti-IGF1-Rα, Santa Cruz rabbit polyclonal 1:1000). The purity of the subcellular fractions was determined by analyzing specific fraction markers: Na, K-ATPase for the membrane fraction (Cell Signalling, rabbit polyclonal 1:1000); GAPDH for the cytosolic fraction (Santa Cruz, rabbit polyclonal 1:1000) and Histone 3 for the nuclear fraction (Cell Signaling, rabbit polyclonal 1:1000). For IGF-1R immunoprecipitation, cardiac myocytes plated in 100 mm dishes were treated with IGF-1 10 nM or control solution for 1 min. After stimulation, cells were scraped and incubated for 15 min on ice using lysis buffer (50 mM HEPES, 1 mM EDTA, 1% Triton X-100, 0.1% SDS, 1 mM Na_3VO_4, 1 mM phenylmethylsulfonyl fluoride, 30 mM $PyroPO_4$, 10 mM NaF, and 1 mg/ml bacitracin). Cell lysates were centrifuged at 14,000 rpm for 30 min to remove insoluble materials. The supernatants (400 µg of total protein) were first pre-cleared with equilibrated protein G sepharose beads (GE Helathcare) and then incubated with 2 µg of anti-IGF-1Rβ antibody (Cell Signaling, rabbit polyclonal) overnight at 4 °C. Immune complexes were precipitated with protein G sepharose beads, washed three times with ice-cold lysis buffer and boiled for 5 min in loading sample buffer. Immunoprecipitated proteins were resolved using NuPAGE bis-tris gels (Invitrogen). Gels were transferred to nitrocellulose membranes (Hybon-C-Super, Amersham) by using a Transblot electro-transfer apparatus (Bio-Rad). For immunoblotting, membranes were blocked with 5% fat-free milk diluted in PBS containing 0,1% tween (PBST) and probed with specified primary antibodies in 2,5% milk diluted in PBST. Blots were then washed and incubated with HRP-conjugated secondary antibodies (Amersham). Immunoreactive bands were detected with Hyperfilm-ECL (Amersham).

Determination of intracellular IP_3 mass: Cardiac myocytes were rinsed and preincubated for 20 min at 37 °C in resting solution (58 mM NaCl, 4.7 mM KCl, 3 mM $CaCl_2$, 1.2 mM $MgSO_4$, 0.5 mM EDTA, 60 mM LiCl, 10 mM glucose, and 20 mM Hepes, pH 7.4). Cells were stimulated by replacement of resting solution with a solution containing 10 nM IGF-1. At the times indicated, the reaction was stopped by rapid aspiration of the stimulating solution, addition of 0.8 M ice-cold perchloric acid and freezing in liquid nitrogen. Samples were allowed to thaw on ice and cell debris was spun down for protein determination. The supernatant was neutralized with a solution of 2 M KOH, 0.1 M MES, and 15 mM EDTA. The neutralized extracts were frozen at -80 °C until required for IP_3 determination. Measurements of IP_3 mass were carried out with a radioligand assay as previously described [12]. Briefly, a crude rat cerebellum membrane preparation was obtained after homogenization of tissue in 50 mM Tris-HCl, pH 7.7, containing 1 mM EDTA, 2 mM β-mercaptoethanol and centrifugation at 20,000 *g* for 15 min. The pellet was resuspended in the same solution containing 0.3 M sucrose and frozen at -80 °C until required for use. The cerebellar membrane preparation was calibrated for IP_3 binding with 1.6 nM [^{3}H]-IP_3 and 2–120 nM of unlabeled IP_3. Sample analysis was performed in a similar way, but replacing unlabeled IP_3 with the neutralized samples. [^{3}H]-IP_3 radioactivity, which remained bound to membranes, was measured in a liquid scintillation spectrometer (Beckman Instruments Corp).

Sucrose gradient fractionation and ^{14}C-cholesterol incorporation: Sucrose gradient fractionation was performed to isolate membranes enriched in lipid rafts, as previously described [13]. Briefly, cardiac myocytes plated on 100 mm culture dishes were tripsinized, centrifuged and resuspended in a solution containing 2.5 mM MES, 150 mM NaCl, 2.0 mM EDTA, 1% triton X-100, pH 6.5, incubated for 20 min on ice and then lysed in the same solution using a Dounce homogenizer. Cellular lysates were centrifuged in sucrose gradients (5%-35%-45%) at 20.000 *g* for 20 h at 4 °C. A total of 12 fractions were collected; the pellet was resuspended in lysis buffer and designated as fraction 13. Equal volumes of all fractions were loaded on NuPAGE bis-tris gels (Invitrogen) and used for Western blot analysis as described above. Alternatively, to determine the distribution of cholesterol in the different fractions, cells were given a pulse of ^{14}C-cholesterol (0,4 mCi/ml in culture medium) for 24 h and then subjected to sucrose fractioning. The amount of cholesterol in 200 ul of each fraction was measured in a liquid scintillation spectrometer (Beckman Instruments Corp).

Acute disruption of T-tubules and lipid rafts: For the acute disruption of T-tubules, a described protocol was performed [14]. Briefly, cardiac myocytes plated on coverslips were washed three times with a control vehicle solution (113 mM NaCl, 5 mM KCl, 1 mM $MgSO_4$, 1 mM $CaCl_2$, 1 mM Na_2HPO_4, 20 mM sodium acetate, 10 mM glucose, 10 mM HEPES and 5 U/l insulin, pH 7.4) and osmotic shock was induced by incubating cells in vehicle solution supplemented with 1.5 M formamide for 20 min at 37 °C. Cells were washed three times and incubated in vehicle solution for 30 min at 37 °C. The cells were loaded with fluo-3AM for Ca^{2+} imaging or fixed and processed for immunofluorescence studies. For the disruption of lipid rafts, cardiac myocytes were washed three times with KRB and then incubated for 30 min in KRB containing 10 mM methyl-β-cyclodextrine at 37 °C (MβCD). Cells were then used for Ca^{2+} imaging or used for the quantification of ^{14}C-cholesterol levels as described above. Alternatively, cells were left in culture medium to recover for 24 h before being used for Ca^{2+} imaging. As controls, MβCD was either incubated after pre-complexing with 10 mM cholesterol for its inactivation, or replaced by the unspecific lipid-binding reagent xylazine (50 μg/ml), according to previously described protocols [15].

Expression of results and statistical analysis: Results are expressed as mean ± s.e.m. Individual groups were compared by Student's *t* test, one-way ANOVA or two-way ANOVA, as indicated. $P<0.05$ was considered the limit of statistical significance.

References

1. Foncea R, Andersson M, Ketterman A, Blakesley V, Sapag-Hagar M, Sugden PH, LeRoith D, Lavandero S. Insulin-like growth factor-I rapidly activates multiple signal transduction pathways in cultured rat cardiac myocytes. *J Biol Chem.* 1997;272(31):19115-19124.
2. Sambrano GR, Fraser I, Han H, Ni Y, O'Connell T, Yan Z, Stull JT. Navigating the signalling network in mouse cardiac myocytes. *Nature.* 2002;420(6916):712-714.
3. Andersson DC, Fauconnier J, Park CB, Zhang SJ, Thireau J, Ivarsson N, Larsson NG, Westerblad H. Enhanced cardiomyocyte Ca(2+) cycling precedes terminal AV-block in mitochondrial cardiomyopathy Mterf3 KO mice. *Antioxid Redox Signal.* 2011;15(9):2455-2464.
4. Zhou YY, Wang SQ, Zhu WZ, Chruscinski A, Kobilka BK, Ziman B, Wang S, Lakatta EG, Cheng H, Xiao RP. Culture and adenoviral infection of adult mouse cardiac myocytes: methods for cellular genetic physiology. *Am J Physiol Heart Circ Physiol.* 2000;279(1):H429-436.
5. Obame FN, Plin-Mercier C, Assaly R, Zini R, Dubois-Rande JL, Berdeaux A, Morin D. Cardioprotective effect of morphine and a blocker of glycogen synthase kinase 3 beta, SB216763 [3-(2,4-dichlorophenyl)-4(1-methyl-1H-indol-3-yl)-1H-pyrrole-2,5-dione], via inhibition of the mitochondrial permeability transition pore. *J Pharmacol Exp Ther.* 2008;326(1):252-258.
6. Westgren M, Ek S, Bui TH, Hagenfeldt L, Markling L, Pschera H, Seiger A, Sundstrom E, Ringden O. Establishment of a tissue bank for fetal stem cell transplantation. *Acta Obstet Gynecol Scand.* 1994;73(5):385-388.
7. Genead R, Danielsson C, Wardell E, Kjaeldgaard A, Westgren M, Sundstrom E, Franco-Cereceda A, Sylven C, Grinnemo KH. Early first trimester human embryonic cardiac Islet-1 progenitor cells and cardiomyocytes: Immunohistochemical and electrophysiological characterization. *Stem Cell Res*. 2010;4(1):69-76.
8. Franceschi RT, Ge C. Gene delivery by adenoviruses. *Methods Mol Biol.* 2008;455:137-147.
9. Koch WJ, Hawes BE, Allen LF, Lefkowitz RJ. Direct evidence that Gi-coupled receptor stimulation of mitogen-activated protein kinase is mediated by G beta gamma activation of p21ras. *Proc Natl Acad Sci U S A.* 1994;91(26):12706-12710.
10. Pusl T, Wu JJ, Zimmerman TL, Zhang L, Ehrlich BE, Berchtold MW, Hoek JB, Karpen SJ, Nathanson MH, Bennett AM. Epidermal growth factor-mediated activation of the ETS domain transcription factor Elk-1 requires nuclear calcium. *J Biol Chem.* 2002;277(30):27517-27527.

11. Varnai P, Balla T. Visualization of phosphoinositides that bind pleckstrin homology domains: calcium- and agonist-induced dynamic changes and relationship to myo-[3H]inositol-labeled phosphoinositide pools. *J Cell Biol.* 1998;143(2):501-510.

12. Bredt DS, Mourey RJ, Snyder SH. A simple, sensitive, and specific radioreceptor assay for inositol 1,4,5-trisphosphate in biological tissues. *Biochem Biophys Res Commun*. 1989;159(3):976-982.

13. Lisanti MP, Scherer PE, Vidugiriene J, Tang Z, Hermanowski-Vosatka A, Tu YH, Cook RF, Sargiacomo M. Characterization of caveolin-rich membrane domains isolated from an endothelial-rich source: implications for human disease. *J Cell Biol.* 1994;126(1):111-126.

14. Brette F, Komukai K, Orchard CH. Validation of formamide as a detubulation agent in isolated rat cardiac cells. *Am J Physiol Heart Circ Physiol.* 2002;283(4):H1720-1728.

15. Huo H, Guo X, Hong S, Jiang M, Liu X, Liao K. Lipid rafts/caveolae are essential for insulin-like growth factor-1 receptor signaling during 3T3-L1 preadipocyte differentiation induction. *J Biol Chem.* 2003;278(13):11561-11569.